nature

https://doi.org/10.1038/s41586-019-1694-1

Supplementary information

The clinical KRAS(G12C) inhibitor AMG 510 drives anti-tumour immunity

In the format provided by the authors and unedited

Jude Canon, Karen Rex, Anne Y. Saiki, Christopher Mohr, Keegan Cooke, Dhanashri Bagal, Kevin Gaida, Tyler Holt, Charles G. Knutson, Neelima Koppada, Brian A. Lanman, Jonathan Werner, Aaron S. Rapaport, Tisha San Miguel, Roberto Ortiz, Tao Osgood, Ji-Rong Sun, Xiaochun Zhu, John D. McCarter, Laurie P. Volak, Brett E. Houk, Marwan G. Fakih, Bert H. O'Neil, Timothy J. Price, Gerald S. Falchook, Jayesh Desai, James Kuo, Ramaswamy Govindan, David S. Hong, Wenjun Ouyang, Haby Henary, Tara Arvedson, Victor J. Cee & J. Russell Lipford

METHODS

Recombinant proteins

Recombinant His-tagged human $KRAS^{G12C/C118A}$ (1-169), GST-human c-RAF (1-149), and His-tagged human $KRAS^{C118A}$ (1-169) were expressed in *Escherichia coli* and purified using affinity and size-exclusion chromatography. Recombinant human SOS1 (564-1049, insect codon optimized) was expressed in *Trichoplusia ni* and purified using affinity and size-exclusion chromatography. A cysteine-light mutant construct was used for co-crystallization studies based on the work of Ostrem et al[1]. Recombinant His-tagged human $KRAS^{G12C/C51S/C80L/C118S}$ (1-169) was expressed in *E. coli* and purified using affinity, ion-exchange, and size-exclusion chromatography, with the His-tag removed for crystallization.

Compounds and antibodies

ARS-1620, PD-0325901[2], trametinib, afatinib, erlotinib, RMC-4550, and AZD5363 were obtained from commercial sources. AMG 511 was synthesized in-house[3]. Syntheses of AMG 510 and its nonreactive propionamide are described in Supplementary Information. For *in vivo* studies, AMG 510 and the MEKi (PD-0325901)[2] were formulated in 2% HPMC, 1% Tween 80 and administered daily via oral gavage at 10 mL/kg. Carboplatin was diluted to 5 mg/mL or 3 mg/mL in 1% PBS and administered by intraperitoneal injection (IP) once per week. The rat anti-mouse PD1 clone 29F.1A12 was chimerized to contain a mouse IgG1 backbone[4], and the Fc receptor silencing mutation N297G was introduced into the IgG heavy chain region to reduce effector function. Anti-PD-1 antibody, 29F.1A12, was diluted in PBS to a concentration of 500 µg/mL and administered once every 3 days by

IP. All antibodies used for immunoblotting, immunohistochemistry, and flow cytometry are listed in Supplementary Table 5.

Cell lines

All cell lines were purchased from American Type Culture Collection (ATCC), except for KM12 and NCI-H3122, which were obtained from the Amgen internal cell bank and originally sourced from the National Cancer Institute (Supplementary Table 1). Cell lines were authenticated by short tandem repeat (STR) profiling or were used immediately after purchase from ATCC. MIA PaCa-2 T2 and SW480-1AC cells were generated by passaging MIA PaCa-2 and SW480 cells, respectively, in mice. CT-26 *KRAS p.G12C* cells were generated from the murine CT-26 colorectal line using CRISPR technology to replace both *KRAS p.G12D* alleles with *p.G12C* (ThermoFisher Scientific). Clone H10 was determined to be homozygous for the *KRAS p.G12C* allele. All cell lines were cultured in RPMI 1640 medium supplemented with 10% fetal bovine serum and penicillin/streptomycin/L-glutamine at 37°C, 5% CO_2 in a humidified incubator.

Synthesis of AMG 510

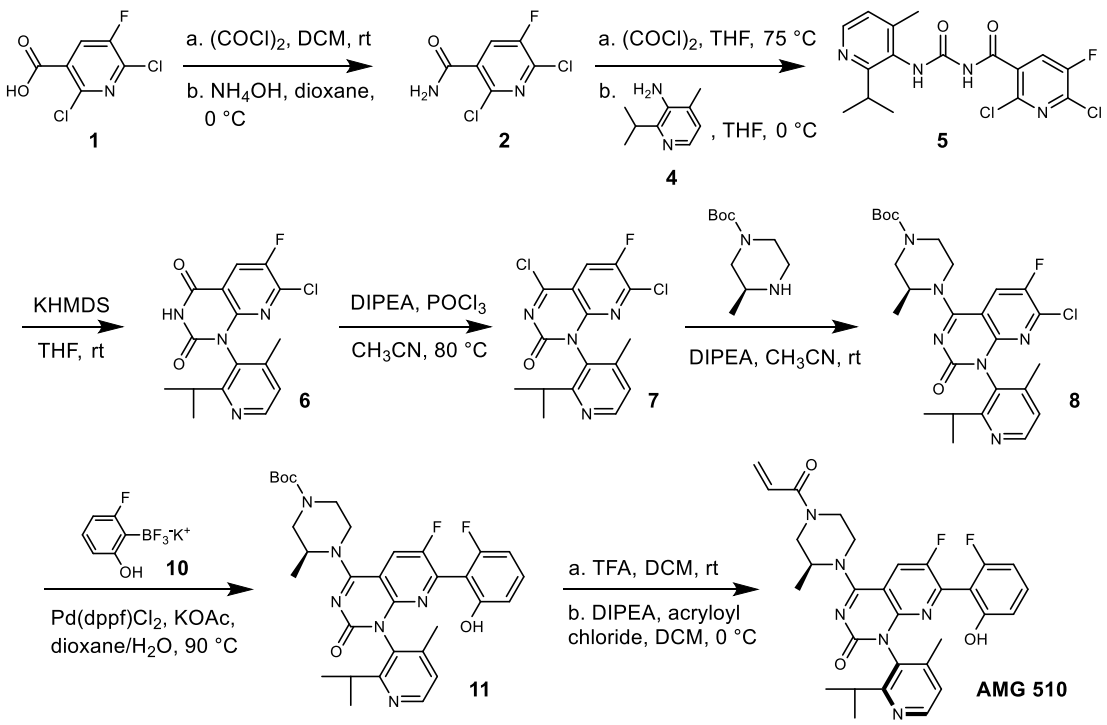

2,6-Dichloro-5-fluoronicotinamide (**2**)**:** Oxalyl chloride (2M solution in DCM, 11.9 mL, 23.8 mmol) and DMF (0.05 mL) were sequentially added to 2,6-dichloro-5-fluoronicotinic acid (**1**; 4.00 g, 19.1 mmol, AstaTech Inc., Bristol, PA) in dichloromethane (48 mL), and the resulting mixture was stirred at ambient temperature for 16 h. The reaction mixture was then concentrated in vacuo, and the residue was dissolved in 1,4-dioxane (48 mL) and cooled to 0°C. Ammonium hydroxide solution (28.0–30% NH_3 basis, 3.6 mL, 28.6 mmol) was slowly added, and the resulting mixture was stirred at 0°C for 30 min. The mixture was then concentrated in vacuo, and the residue was diluted with 1:1 EtOAc/heptane, agitated for 5 min, and filtered. The filtrate was concentrated to half-volume and re-filtered. The combined collected solids were washed with heptane and dried overnight in a reduced-pressure oven (45°C) to provide **2** (2.0 g, 50% yield). ^{1}H-

NMR (400 MHz, DMSO-d_6): δ 8.23 p.p.m (d, J = 7.9 Hz, 1H), 8.09 (br s, 1H), 7.93 (br s, 1H); ^{19}F-NMR (376 MHz, DMSO-d_6): δ –122.39 (s, 1F); *m/z* (ESI, +ve ion): 208.9 $(M+H)^+$.

2,6-Dichloro-5-fluoro-*N*-((2-isopropyl-4-methylpyridin-3-yl)carbamoyl)nicotinamide (**5**)**:** To an ice-cooled slurry of **2** (5.00 g, 23.9 mmol) in THF (20 mL) was slowly added oxalyl chloride (2 M solution in DCM, 14.4 mL, 28.8 mmol). The resulting mixture was heated at 75°C for 1 h, then allowed to cool and concentrated in vacuo to half volume. The concentrate was cooled to 0°C and diluted with THF (20 mL), and a solution of **4** (3.59 g, 23.9 mmol) in THF (10 mL) was added dropwise via cannula. The resulting mixture was stirred at 0°C for 1 h, then diluted with a 1:1 mixture of brine and saturated aqueous ammonium chloride and extracted with EtOAc (3x). The combined extracts were dried over anhydrous sodium sulfate and concentrated in vacuo to provide **5**, which was used without further purification. *m/z* (ESI, +ve ion): 385.1 $(M+H)^+$.

7-Chloro-6-fluoro-1-(2-isopropyl-4-methylpyridin-3-yl)pyrido[2,3-*d*]pyrimidine-2,4(1H,3H)-dione (**6**)**:** To an ice-cooled solution of **5** (9.20 g, 24.0 mmol) in THF (40 mL) was slowly added KHMDS (1 M solution in THF, 50.2 mL, 50.2 mmol). The ice bath was removed, and the resulting mixture was stirred at room temperature for 40 min. Saturated aqueous ammonium chloride was added, and the resulting mixture was extracted with EtOAc (3x). The combined extracts were dried over anhydrous sodium sulfate and concentrated in vacuo. Chromatographic purification of the residue (silica gel; eluent: 0–50% EtOAc-EtOH (3:1)/heptane) provided **6** (9.24 g, quantitative yield). ^{1}H-NMR (400 MHz, DMSO-d_6): δ 12.27 p.p.m. (br s, 1H), 8.48–8.55 (m, 2H), 7.29 (d, J = 4.8 Hz, 1H), 2.87 (quin, J = 6.6 Hz, 1H), 1.99–2.06 (m, 3H), 1.09 (d, J = 6.6 Hz, 3H),

1.01 (d, *J* = 6.6 Hz, 3H); ^{19}F-NMR (376 MHz, DMSO-d_6): δ –126.90 (s, 1F); *m/z* (ESI, +ve ion): 349.1 $(M+H)^+$.

4,7-Dichloro-6-fluoro-1-(2-isopropyl-4-methylpyridin-3-yl)pyrido[2,3-*d*]pyrimidin-2(1H)-one (**7**)**:** Phosphorus oxychloride (1.63 mL, 17.5 mmol) was added, dropwise, to a solution of **6** (4.70 g, 13.5 mmol) and DIPEA (3.50 mL, 20.2 mmol) in acetonitrile (20 mL), and the resulting mixture was heated at 80°C for 1 h, then cooled to room temperature and concentrated in vacuo to provide **7**, which was used without further purification. *m/z* (ESI, +ve ion): 367.1 $(M+H)^+$.

(*S*)-*tert*-Butyl 4-(7-chloro-6-fluoro-1-(2-isopropyl-4-methylpyridin-3-yl)-2-oxo-1,2-dihydropyrido[2,3-*d*]pyrimidin-4-yl)-3-methylpiperazine-1-carboxylate (**8**)**:** To an ice-cooled solution of **7** (13.5 mmol) in acetonitrile (20 mL) was added DIPEA (7.1 mL, 40.3 mmol), followed by (*S*)-4-*N*-Boc-2-methyl piperazine (3.23 g, 16.1 mmol, Combi-Blocks, Inc., San Diego, CA). The resulting mixture was warmed to room temperature and stirred for 1 h, then diluted with cold saturated aqueous sodium bicarbonate (200 mL) and EtOAc (300 mL). The mixture was stirred for an additional 5 min, and the organic layer was collected. The aqueous layer was extracted with additional EtOAc (1x), and the combined organic extracts were dried over anhydrous sodium sulfate and concentrated in vacuo. Chromatographic purification of the residue (silica gel; eluent: 0–50% EtOAc/heptane) gave **8** (5.71 g, 80% yield). ^{1}H-NMR (400 MHz, DMSO-d_6): δ 8.45–8.51 p.p.m. (1 H, m), 8.31–8.41 (1 H, m), 7.23–7.29 (1 H, m), 4.67–5.01 (1 H, m), 4.09–4.25 (1 H, m), 3.88–4.07 (1 H, m), 3.78–3.87 (1 H, m), 3.59–3.74 (1 H, m), 3.04–3.21 (2 H, m), 2.59–2.66 (1 H, m), 1.88–1.98 (3 H, m), 1.43–1.50 (9 H, m), 1.27–1.35 (3 H, m), 1.03–1.10 (3 H, m), 0.94–1.03 (3 H, m); *m/z* (ESI, +ve ion): 531.2 $(M+H)^+$.

(3*S*)-*tert*-Butyl 4-(6-fluoro-7-(2-fluoro-6-hydroxyphenyl)-1-(2-isopropyl-4-methylpyridin-3-yl)-2-oxo-1,2-dihydropyrido[2,3-*d*]pyrimidin-4-yl)-3-methylpiperazine-1-carboxylate (**11**)**:** A mixture of **8** (4.3 g, 8.1 mmol), **10** (2.9 g, 10.5 mmol), potassium acetate (3.2 g, 32.4 mmol), and [1,1′-bis(diphenylphosphino)ferrocene]dichloropalladium(II), complex with dichloromethane (661 mg, 0.81 mmol) in 1,4-dioxane (80 mL) was sparged with nitrogen for 1 min. De-oxygenated water (14 mL) was added, and the resulting mixture was heated at 90°C for 1 h, then cooled to room temperature, diluted with half-saturated aqueous sodium bicarbonate, and sequentially extracted with EtOAc (2x) and DCM (1x). The combined extracts were dried over anhydrous sodium sulfate and concentrated in vacuo. Chromatographic purification of the residue (silica gel; eluent: 0–60% EtOAc-EtOH (3:1)/heptane) furnished **11** (4.52 g, 92% yield). ^{1}H-NMR (400 MHz, DMSO-d_6): δ 10.19 p.p.m. (br s, 1H), 8.38 (d, J = 5.0 Hz, 1H), 8.26 (dd, J = 12.5, 9.2 Hz, 1H), 7.23–7.28 (m, 1H), 7.18 (d, J = 5.0 Hz, 1H), 6.72 (d, J = 8.0 Hz, 1H), 6.68 (t, J = 8.9 Hz, 1H), 4.77–4.98 (m, 1H), 4.24 (br t, J = 14.2 Hz, 1H), 3.93–4.08 (m, 1H), 3.84 (br d, J=12.9 Hz, 1H), 3.52–3.75 (m, 1H), 3.07–3.28 (m, 1H), 2.62–2.74 (m, 1H), 1.86–1.93 (m, 3H), 1.43–1.48 (m, 9H), 1.35 (dd, J = 10.8, 6.8 Hz, 3H), 1.26–1.32 (m, 1H), 1.07 (dd, J = 6.6, 1.7 Hz, 3H), 0.93 (dd, J = 6.6, 2.1 Hz, 3H); ^{19}F-NMR (376 MHz, DMSO-d_6): δ –115.65 (s, 1F), –128.62 (s, 1F); *m/z* (ESI, +ve ion): 607.3 $(M+H)^+$.

(1*R*)-6-Fluoro-7-(2-fluoro-6-hydroxyphenyl)-1-[4-methyl-2-(1-methylethyl)-3-pyridinyl]-4-[(2*S*)-2-methyl-4-(1-oxo-2-propen-1-yl)-1-piperazinyl]-pyrido[2,3-d]pyrimidin-2(1*H*)-one (**AMG 510**): Trifluoroacetic acid (25 mL, 324 mmol) was added to a solution of **11** (6.30 g, 10.4 mmol) in DCM (30 mL), and the resulting mixture was stirred at room temperature for 1 h. The mixture was then concentrated in vacuo, and the residue was

taken up in DCM (30 mL), cooled to 0°C, and sequentially treated with DIPEA (7.3 mL, 41.7 mmol) and a solution of acryloyl chloride (0.849 mL, 10.4 mmol) in DCM (3 mL; added dropwise). The resulting mixture was stirred at 0°C for 10 min, then diluted with half-saturated aqueous sodium bicarbonate and extracted with DCM (2x). The combined extracts were dried over anhydrous sodium sulfate and concentrated in vacuo. Chromatographic purification of the residue (silica gel; eluent: 0–100% EtOAc-EtOH (3:1)/heptane) followed by chiral resolution using supercritical fluid chromatography (Chiralpak IC, 30 × 250 mm, 5 µm, 55% MeOH/CO_2, 120 mL/min, 102 bar; first-eluting peak collected) provided **AMG 510** (2.25 g, 43% yield). ^{1}H-NMR (600 MHz, DMSO-d_6) δ ppm 10.20 (s, 1H), 8.39 (d, *J* = 4.9 Hz, 1H), 8.30 (d, *J* = 8.9 Hz, 0.5H), 8.27 (d, *J* = 8.7 Hz, 0.5H), 7.27 (q, *J* = 8.4 Hz, 1H), 7.18 (d, *J* = 4.9 Hz, 1H), 6.87 (dd, *J* = 16.2, 10.8 Hz, 0.5H), 6.84 (dd, *J* = 16.2, 10.7 Hz, 0.5H), 6.74 (d, *J* = 8.4 Hz, 1H), 6.68 (t, *J* = 8.4 Hz, 1H), 6.21 (d, *J* = 16.2 Hz, 0.5H), 6.20 (d, *J* = 16.2 Hz, 0.5H), 5.76 (d, *J* = 10.8 Hz, 0.5H), 5.76 (d, *J* = 10.7 Hz, 0.5H), 4.91 (m, 1H), 4.41 (d, *J* = 12.2 Hz, 0.5H), 4.33 (d, *J* = 12.2 Hz, 1H), 4.28 (d, *J* = 12.2 Hz, 0.5H), 4.14 (d, *J* = 12.2 Hz, 0.5H), 4.02 (d, *J* = 13.6 Hz, 0.5H), 3.69 (m, 1H), 3.65 (d, *J* = 13.6 Hz, 0.5H), 3.52 (t, *J* = 12.2 Hz, 0.5H), 3.27 (d, *J* = 12.2 Hz, 0.5H), 3.15 (t, *J* = 12.2 Hz, 0.5H), 2.72 (m, 1H), 1.90 (s, 3H), 1.35 (d, *J* = 6.7 Hz, 3H), 1.08 (d, *J* = 6.7 Hz, 3H), 0.94 (d, *J* = 6.7 Hz, 3H); ^{19}F-NMR (376 MHz, DMSO-d_6): *δ* –115.6 (s, *J* = 5.2 Hz, 1F), –128.6 (br. s, 1F); ^{13}C-NMR (151 MHz, DMSO-d_6) δ ppm 165.0 (1C), 163.4 (1C), 162.5 (1C), 160.1 (1C), 156.8 (1C), 153.7 (1C), 151.9 (1C), 149.5 (1C), 148.3 (1C), 145.2 (1C), 144.3 (1C), 131.6 (1C), 130.8 (1C), 127.9 (0.5C), 127.9 (0.5C), 127.8 (0.5C), 127.7 (0.5C), 123.2 (1C), 122.8 (1C), 111.7 (1C), 109.7 (1C), 105.7 (1C), 105.3 (1C), 51.4 (0.5C), 51.0 (0.5C),

48.9 (0.5C), 45.4 (0.5C), 44.6 (0.5C), 43.7 (0.5C), 43.5 (0.5C), 41.6 (0.5C), 29.8 (1C), 21.9 (1C), 21.7 (1C), 17.0 (1C), 15.5 (0.5C), 14.8 (0.5C); *m/z* (ESI, +ve ion): 561.2 $(M+H)^+$.

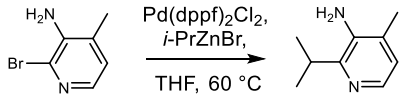

3 **4**

2-Isopropyl-4-methylpyridin-3-amine (**4**)**:** [1,1′-bis(diphenylphosphino)ferrocene]dichloropalladium(II), complex with dichloromethane (79 mg, 0.10 mmol) was added to a slurry of 3-amino-2-bromo-4-picoline (**3**; 360 mg, 1.9 mmol, Combi-Blocks, San Diego, CA) in THF (4 mL), and the resulting mixture was sparged with argon for 2 min. 2-Propylzinc bromide (0.5 M solution in THF, 5.40 mL, 2.7 mmol) was added, and the resulting solution was heated at 60°C for 17 h, then allowed to cool to room temperature. Water (10 mL) and 1 N aqueous NaOH (20 mL) were added, and the resulting mixture was extracted with EtOAc (2x). The combined organic layers were dried over anhydrous sodium sulfate and concentrated in vacuo. Chromatographic purification of the residue (silica gel, eluent: 0–15% MeOH/DCM) furnished **4** (284 mg, 98% yield). ^{1}H-NMR (400 MHz, DMSO-d_6): δ 7.66 p.p.m. (d, J = 4.6 Hz, 1H), 6.78 (d, J = 4.8 Hz, 1H), 4.72 (br s, 2H), 3.14–3.25 (m, 1H), 2.08 (s, 3H), 1.14 (d, J = 6.8 Hz, 6H); *m/z* (ESI, +ve ion): 151.1 $(M+H)^+$.

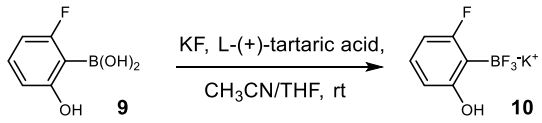

(2-Fluoro-6-hydroxyphenyl)potassium trifluoroborate (**10**)**:** A solution of potassium fluoride (44.7 g, 770 mmol) in water (75 mL) was added to a suspension of (2-fluoro-6-hydroxyphenyl)boronic acid (**9**; 30 g, 192 mmol, Combi-Blocks, San Diego, CA) in acetonitrile (750 mL). After 2 min of stirring, a solution of L-(+)-tartaric acid (72.2 g, 481 mmol) in THF (375 mL) was added over 10 min. The resulting mixture was mechanically stirred for 1 h. Suspended solids were removed by filtration and washed with a small amount of THF. The combined filtrate was then partially concentrated in vacuo until solids began to precipitate. The filtrate was cooled to –20°C and stirred for 16 h, then slowly warmed to ambient temperature. 2-Propanol (20 mL) was added, and the precipitated solids were collected by filtration and washed with 2-propanol to provide 27.5 g of solid. The filtrate was again partially concentrated (until precipitation observed), cooled to –20°C, and stirred for 20 min. Additional 2-propanol was added, and the precipitated solid was collected by filtration and washed with 2-propanol. The two batches of solid were combined to provide **10** (34.6 g, 82% yield). ^{1}H-NMR (400 MHz, DMSO-d_6): δ 8.07 p.p.m. (q, J = 14.7 Hz, 1H), 6.93 (q, J = 7.5 Hz, 1H), 6.30–6.38 (m, 2H).

Synthesis of AMG 510 propionamide

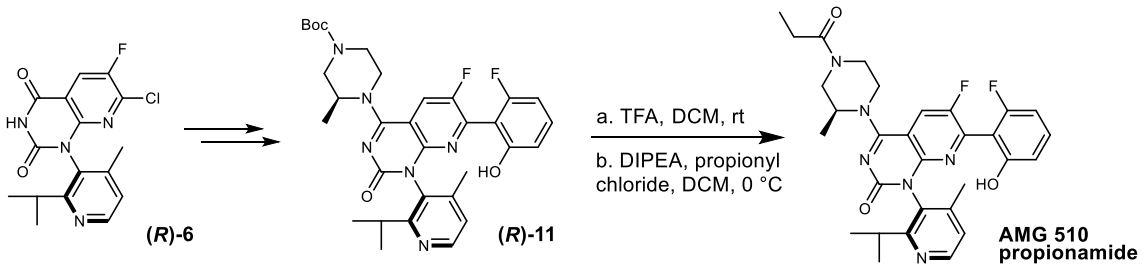

(*R*)-6 & **(*R*)-11:** Racemic **6** was resolved by supercritical fluid chromatography (Chiralpak AD, 21 × 250 mm, 5 µm, 40% MeOH/CO_2, 80 mL/min, 110 bar; second-eluting peak collected) to provide **(*R*)-6**, which was converted to **(*R*)-11** using the procedures reported for racemic substrates.

(1*R*)-6-Fluoro-7-(2-fluoro-6-hydroxyphenyl)-1-(4-methyl-2-(2-propanyl)-3-pyridinyl)-4-((2*S*)-2-methyl-4-propanoyl-1-piperazinyl)pyrido[2,3-*d*]pyrimidin-2(1H)-one (**AMG 510 propionamide**)**:** Trifluoroacetic acid (4.0 ml, 51.9 mmol) was added to a solution of **(*R*)-11** (0.196 g, 0.323 mmol) in DCM (5 mL), and the resulting mixture was stirred at room temperature for 20 min. The mixture was then concentrated in vacuo, and the residue was taken up in DCM (10 mL), cooled to 0°C, and sequentially treated with DIPEA (0.169 mL, 0.969 mmol) and propionyl chloride (0.016 mL, 0.194 mmol). The resulting mixture was stirred at 0°C for 10 min, then diluted with saturated aqueous sodium bicarbonate and extracted with DCM (2x). The combined extracts were dried over anhydrous sodium sulfate and concentrated in vacuo. Chromatographic purification of the residue (silica gel; eluent: 0–70% EtOAc-EtOH (3:1)/heptane) provided **AMG 510 propionamide** (0.180 g, 99% yield). ^{1}H-NMR (400 MHz, DMSO-d_6): δ 10.20 p.p.m (s, 1H), 8.40 (d, J=5.0 Hz, 1H), 8.27 (br dd, J=15.1, 9.3 Hz, 1H), 7.27 (m,

1H), 7.21 (br d, J=4.8 Hz, 1H), 6.73 (d, J=8.3 Hz, 1H), 6.69 (t, J=8.9 Hz, 1H), 4.87 (br s, 1H), 4.31 (m, 1.5H), 4.21 (br d, J=13.5 Hz, 0.5H), 3.94 (br d, J=12.2 Hz, 0.5H), 3.82 (br d, J=13.3 Hz, 0.5H), 3.62–3.76 (m, 1H), 3.52–3.62 (m, 0.5H), 3.43–3.51 (m, 0.5H), 3.18 (br dd, J=13.3, 3.3 Hz, 0.5H), 3.06 (br t, J=10.7 Hz, 0.5H), 2.73 (br dd, J=10.5, 6.1 Hz, 1H), 2.33–2.48 (m, 2H), 1.91 (s, 3H), 1.29–1.42 (m, 3H), 0.98–1.12 (m, 6H), 0.94 (d, J=6.6 Hz, 3H); *m/z* (ESI, +ve ion): 563.2 $(M+H)^+$.

X-ray crystallography

Purified un-tagged $KRAS^{G12C/C51S/C80L/C118S}$ ("KRAS") in 20 mM HEPES pH 7.5, 150 mM NaCl was concentrated to 40 mg/mL and added to a two-fold molar excess of solid AMG 510 compound dissolved in DMSO. Co-crystallization was performed using sitting drop vapor diffusion method. "KRAS"-AMG 510 protein-complex sample and crystallization buffer (1 mM $MgCl_2$, 0.1 M MES pH 6.5, 30% w/v polyethylene glycol 4000) were mixed 1:1. Crystals appeared in one day at 20°C.

The data set was collected on a Pilatus 6M silicon pixel detector at the Advanced Light Source Beamline 5.0.1 at wavelength 0.97741 Å and temperature 100K. The data were integrated and scaled using HKL2000[5]. The structure was solved by molecular replacement using MolRep[6,7], with an apo KRAS structure as a search model. There is one protein molecule in the asymmetric unit. The structure was refined using Refmac5[6,8], and model building was performed using the graphics program Coot[9]. The ligand was generated using PRODRG[10]. The structure of $KRAS^{G12C/C51S/C80L/C118S}$ bound to GDP and AMG 510 was refined to 1.65Å with an R-factor of 18.1% and R_{free} of 21.5%. Ramachandran statistics were 98.2% favored, 1.8% allowed, with no outliers. Amino acid residues 105-107 were unresolved in the crystal structure. While the relative orientation

of the fluoro- and hydroxyl-substituents of the terminal aromatic ring of AMG 510 could not be uniquely determined from the ligand electron density alone, we observed that the protein environment was significantly different on each side of the aromatic ring. Therefore, in the deposited coordinates, the fluoro-substituent was chosen to occupy the more hydrophobic environment and hydroxyl-substituent was chosen to occupy the more hydrophilic environment, with the hydroxyl-substituent within hydrogen-bonding distance of the D63 backbone carbonyl. The X-ray crystallographic coordinates and structure factor files have been deposited in the Protein Data Bank (PDB ID code: 6OIM; Extended Data Table 1). Figures were generated using the PyMOL Molecular Graphics System, version 2.1.1 (Schrödinger, LLC).

Coupled nucleotide exchange assays

Inhibition of the SOS1-catalyzed nucleotide exchange activity of $KRAS^{G12C/C118A}$ or $KRAS^{C118A}$ was measured using Alpha technology (PerkinElmer). 20 nM GDP-bound human $KRAS^{G12C/C118A}$ or $KRAS^{C118A}$ protein was incubated with serially-diluted AMG 510 or DMSO for 5 min at RT in reaction buffer (25 mM HEPES, pH 7.4; 10 mM $MgCl_2$; 0.01% Triton X-100). The wildtype cysteine at position 118 was changed to alanine so that the only reactive cysteine available was at position 12. For all subsequent steps, DTT was added to the reaction buffer at a final concentration of 1 mM. Next, GTP and SOS-1 were added in DTT-reaction buffer at final concentrations of 1.25 mM or 500 nM, respectively, and incubated at RT for 30 min. Finally, c-RAF RBD (50 nM final), Alpha glutathione donor beads (PerkinElmer; 20 μg/mL final), and AlphaLISA® nickel chelate acceptor beads (PerkinElmer; 20 μg/mL final), all diluted in DTT-reaction buffer, were added. The reaction mixture was incubated at RT for 5 min, and the plates were read on an EnVision®

Multilabel Reader. Luminescence signal was measured at 570 nm following a 180 ms excitation at 680 nm. Signal intensity was normalized to DMSO control.

ERK1/2 phosphorylation (p-ERK) assays

For cellular assays, 2.5E+04 cells/well were seeded in 96-well plates and incubated at 37°C, 5% CO_2 for 16 hours. Serially-diluted compound or DMSO was added to the cells, and the plates were incubated at 37°C, 5% CO_2 for two hours. Following treatment, the cells were washed with ice-cold PBS and lysed in RIPA lysis buffer (50 mM Tris-HCl, pH 7.5; 1% Igepal; 0.5% sodium deoxycholate; 150 mM NaCl; 0.1% sodium dodecyl sulfate) containing protease and phosphatase inhibitors. Basal ERK1/2 phosphorylation (p-ERK) levels were measured in treated cell lysates using phospho-ERK1/2 whole cell lysate kits (Meso Scale Discovery) according to the manufacturer's protocol. Signal intensity was normalized to DMSO control.

For tumor cell lysates from *in vivo* pharmacodynamic assays, samples were analyzed using phospho-ERK1/2 and total ERK1/2 whole cell lysate kits (Meso Scale Discovery) according to the manufacturer's protocol. Phospho-ERK1/2 signal was normalized to total ERK1/2 signal for a given sample, and percent inhibition of p-ERK was calculated relative to the vehicle group.

Cell viability assays

For adherent viability assays, 0.5-1.0E+03 cells/well were seeded in 384-well plates (or 2.5-4.0E+04 cells/well in 96-well plates) and incubated at 37°C, 5% CO_2 for 16 hours. Serially-diluted compound or DMSO was added to the cells, and plates were incubated at 37°C, 5% CO_2 for 72 hours. Cell viability was measured using a CellTiter-Glo®

Luminescent Cell Viability Assay kit (Promega) according to the manufacturer's protocol. The luminescence signal of treated samples was normalized to DMSO control.

For spheroid viability assays, 2.5-4.0E+04 cells/well were seeded in 96-well spheroid microplates (Corning) and incubated at 37°C, 5% CO_2 for 24 hours. The same procedure was followed as described above, except viability was measured using a CellTiter-Glo® 3D Cell Viability Assay kit (Promega) according to the manufacturer's protocol.

Synergistic combination studies

Combination experiments to assess synergistic interactions of AMG 510 with other inhibitors *in vitro* were carried out as previously described[11].

Kinetic analyses

Formation of covalent inhibitor-$KRAS^{G12C}$ adducts was measured using MS as previously described[12]. Relative percent bound values for various inhibitor concentrations over a time course were fit to an exponential equation to generate k_{obs} values for each concentration tested using Prism (GraphPad Software). The resulting k_{obs} values were then replotted versus inhibitor concentration to generate k_{inact} and K_i values.

To determine the kinetic values of covalent inhibitor-$KRAS^{G12C}$ adduct formation in cells, basal p-ERK levels were measured following treatment with serially-diluted inhibitors over a time course exactly as described above, and percent activity values were used for the kinetic calculations. Similarly, basal p-ERK levels were measured following treatment with 2.5 µM RMC-4550 over a time course to estimate the GTP-hydrolysis rate of $KRAS^{G12C}$.

AMG 510-KRAS^{G12C} conjugate detection

Anti-human RAS (anti-RAS; Abcam) antibody was biotinylated with EZ-Link NHS-PEG4-Biotin (ThermoFisher Scientific) using the manufacturer's protocol. Residual biotin was removed, and the resulting biotin-anti-RAS was loaded onto Dynabeads® MyOne™ Streptavidin C1 beads (ThermoFisher Scientific) for an hour at RT with shaking. Lysates from *in vitro*-treated cells or *in vivo*-treated tumor cells described previously were incubated with biotinylated anti-RAS beads for three hours at RT with shaking. Using a magnet, beads were washed with PBST, followed by PBS, and then water. Samples were eluted from the beads using 2% aqueous formic acid/10% aqueous acetonitrile (ACN), followed by incubation at RT with shaking for 10 min. The supernatant was transferred to a 96-well plate and dried. Samples were resuspended in a denaturation buffer (10 mM TCEP, 8 M urea) and incubated at 65°C with shaking for 15 min. Iodoacetamide (40 mM) was added and incubated at 37°C for 30 min, protected from light. 50 mM NH_4HCO_3 and trypsin (0.01 µg/µL) were added, and samples were digested overnight at 37°C for ~16–20 hours, then quenched with formic acid to give a final concentration of 1% (v:v). Samples were analyzed by liquid chromatography-tandem mass spectrometry (LC-MS/MS) by multiple reaction monitoring (MRM) in positive ion electrospray mode using a 6500 QTRAP (AB SCIEX) coupled to an Acquity UPLC (Waters). Samples were injected onto an Acquity UPLC BEH C8 1.7μm, 2.1 x 100 mm column (Waters). The mobile phases consisted of A (water + 0.1% formic acid) and B (acetonitrile + 0.1% formic acid). The LC gradient was 5-50% B in 5 min, 50-95% B in 0.5 min, and 95% B in 1 minute. The KRAS^{G12C} LVVVGAC(CAM)GVGK (529.8 → 846.3) and AMG 510-modifed KRAS^{G12C} AMG 510-LVVVGACGVGK (521.4 → 675.2) peptides were monitored. Occupancy was

calculated as a percentage of AMG 510-modified $KRAS^{G12C}$ peptide normalized to the sum of unmodified and modified $KRAS^{G12C}$ peptide.

Cysteine proteomic analysis

Human non-small cell lung cancer NCI-H358 cells were seeded at 2.0E+06 cells/10 cm plate and incubated at 37°C, 5% CO_2 for 16 hours. The cells were then treated with 1 µM AMG 510 or DMSO (*n*=5) and incubated at 37°C, 5% CO_2 for four hours. Cells were then washed with ice-cold PBS containing protease inhibitors and removed from the plates. Snap-frozen cell pellets were processed at IQ Proteomics, LLC by mass spectrometry (MS) according to their protocol as well as that described by Patricelli et al[13]. Briefly, cell pellets were lysed and treated with 100 µM desthiobiotin iodoacetamide to label remaining unreacted solvent exposed cysteines. Following trypsin digestion, the peptide mixture generated from each sample was labeled with TMT-10 plex (Tandem Mass Tag) isobaric label reagents (ThermoFisher Scientific). After labeling, the samples were mixed prior to enrichment of the desthiobiotinylated peptides using high-capacity streptavidin agarose. The enriched peptides were analyzed by nano-LC-MS using a three-hour gradient and synchronous precursor selection (SPS)-based MS3 method on an Orbitrap Lumos mass spectrometer (ThermoFisher Scientific)[14-16]. Identification of desthiobiotinylated peptides was obtained using database searching parameters listed in Supplementary Table 2. All data processing for statistical analysis was performed in Microsoft Excel using normalized peak abundances of the cysteine-containing peptides. Log_2-fold changes were calculated between DMSO control and AMG 510-treated sample groups. A two-tailed t test for each peptide was performed to assess the statistical significance of difference between treated and DMSO control sample groups assuming equal variance. A volcano plot showing

negative $\log_{10}$ p-values was plotted against the $\log_2$-fold changes for each desthiobiotinylated cysteine-containing peptide. Peptides which displayed a $\log_2$-fold decrease in abundance greater than 2 and a p-value <0.0001 were designated as covalent targets of AMG 510 (*n*=5 biological replicates).

Immunoblot analyses

MIA PaCa-2 or NCI-H358 cells were plated at a density of 5.0E+05 cells/well in 6-well plates and incubated at 37°C, 5% CO_2 for 16 hours. AMG 510 was serially diluted and added to appropriate wells to a final concentration of 1 μM, 0.1 μM, 0.01 μM, or 0.001 μM in 0.1% DMSO. Plates were incubated at 37°C, 5% CO_2 for the indicated times. At each time point, plates were removed from the incubator and placed on ice. The cells were washed with ice-cold PBS, scraped off the plates, pelleted by centrifugation, and lysed in RIPA buffer (50 mM Tris-HCl, pH 7.5; 1% Igepal; 0.5% sodium deoxycholate; 150 mM NaCl; 0.1% sodium dodecyl sulfate) containing cOmplete™, EDTA-free protease inhibitor (Roche) and PhosSTOP™ phosphatase inhibitor (Roche).

Protein concentrations were determined using DC Protein Assay (Bio-Rad). Proteins were separated by electrophoresis using NuPAGE Bis-Tris gels (ThermoFisher Scientific) and transferred to PVDF membranes (ThermoFisher Scientific) according to standard protocols. Membranes were immunoblotted with the primary antibodies listed in Supplementary Table 5 in TBST containing either 5% milk or 5% bovine serum albumin and incubated at 4°C for 16-20 h. Membranes were then incubated with donkey anti-rabbit IgG HRP antibody conjugate (GE Healthcare) and developed using either SuperSignal West Pico or SuperSignal West Femto (ThermoFisher Scientific) according to the manufacturer's protocol. Chemiluminescent images of the immunoblots were

captured using a Bio-Rad ChemiDoc with ImageLab software (v4.1 or v5.2.1). To detect β-actin, the RAS membrane was reprobed with anti-β-actin HRP antibody, developed, and imaged as described above.

Stable isotope labeling by amino acids in cell culture (SILAC)

Light Medium (LM) was prepared by adding the following components to final volume of 1 L: 100 mL dialyzed FBS, 10.4 g powdered RPMI-1640 medium, 2 g sodium bicarbonate, 200 mg L-arginine, 48 mg L-lysine, 100 mg L-leucine, and 1x Pen-Strep, which was filtered with 0.22 µm filter system. Heavy Medium (HM) was prepared identically to LM, but 100 mg [$^{13}C_6$]-L-leucine (Cambridge Isotope Laboratories) was substituted for the non-isotopically enriched L-leucine. MIA PaCa-2 and NCI-H358 cells were seeded (3.0E+05 cells) into T75 flasks with LM; LM was changed daily. After 48 hours, the cells were washed with 1x PBS, and the media was switched to HM; HM was changed daily for 4 days. On Day 6, the cells were washed with 1x PBS and the media was switched to LM; LM was changed daily. Starting on Day 6, the MIA PaCa-2 samples were collected at 0, 1, 3, 6, 9, 12, 15, 18, 21, 24, 30, 36, 48, and 72 h. Starting on Day 6, the NCI-H358 samples were collected at 0, 3, 6, 9, 12, 24, 36, 48, 72, and 96 h. Separate T75 flasks, prepared in triplicate were collected at each timepoint and processed to lysates.

T75 flasks were washed with 1x PBS, treated with trypsin and incubated for 2 min followed by the addition of ice-cold PBS containing 10% dialyzed FBS. Cells were mixed and collected, followed by cell counting using a Vi-CELL XR. The remaining cells were centrifuged and washed with ice-cold PBS (no Mg^{+2}, no Ca^{+2}). Cells were centrifuged again, PBS was removed, and the cells were lysed in a small volume of ice-cold RIPA containing phosphatase (PhosSTOP, Roche) and protease (cOmplete EDTA-free,

Roche) inhibitors. Resulting lysates were vortexed, put on ice for 10 min, centrifuged to remove insoluble debris, and then stored at −80°C until further processing.

To determine the half-life of SILAC KRAS^{G12C}, the protocol for AMG 510-KRAS^{G12C} conjugate detection was used essentially as described above, with the following exceptions: incubation with biotin-anti-RAS plus Dynabeads® MyOne™ Streptavidin C1 beads for 1.5 h; incubation of lysates with biotinylated anti-RAS beads for 2 h; washing of beads with PBST, followed by PBS; elution of samples using 3% aqueous formic acid/30% aqueous acetonitrile; incubation of resuspended samples at 37°C for 1 h using a water bath; incubation with iodoacetamide at 25°C for 1 h; digestion with 50 mM NH_4HCO_3 and trypsin (0.1 µg/µL) at 37°C for 24 hours; and concentration of samples to a volume of approximately 80 µL before analysis by mass spectrometry. Samples were analyzed by liquid chromatography-tandem mass spectrometry (LC-MS/MS) by multiple reaction monitoring (MRM) in positive ion electrospray mode using a 6500 QTRAP (AB SCIEX) coupled to an Acquity UPLC (Waters) as described above. The following peptides for KRAS^{G12C} (LVVVGAC(CAM)GVGK (529.8 → 846.3) & ^{13}C-LVVVGAC(CAM)GVGK (532.8 → 846.3)) and RAS WT (LVVVGAGGVGK (478.3 → 743.2) & ^{13}C-LVVVGAGGVGK (481.3 → 743.2)) were used to monitor the transition from heavy to light labeling. The Relative Isotope Abundance (RIA) was determined using the following formula:

$$\mathrm{RIA} = \frac{\mathrm{A_{heavy}}}{\mathrm{A_{light}} + \mathrm{A_{heavy}}}$$

To account for the impact of cell growth on the determination of protein half-life, cell numbers and RIA data associated with each timepoint were simultaneously fit to a series of equations to determine the half-life of $KRAS^{G12C}$ in MIA PaCa-2 and NCI-H358 cells. The following equations were used:

First order equation for heavy peptide:

$$\frac{\mathrm{d\,Hv}}{\mathrm{dt}} = -\mathrm{k_{dec}\,Hv}$$

First order equation for light peptide:

$$\frac{\mathrm{d\,lt}}{\mathrm{dt}} = \mathrm{k_{dec}\,(Hv_0 + lt_0)} - \mathrm{k_{dec}\,lt} + \frac{\mathrm{cell_{new}}}{\mathrm{cell_{(0)}}}\,\mathrm{(Hv_0 + lt_0)\,k_{dec}} - \mathrm{k_{dec}}\,\frac{\mathrm{cell_{new}}}{\mathrm{cell_{(0)}}}\,\mathrm{lt}$$

First order equation for cell growth:

$$\frac{\mathrm{d\,cell_{new}}}{\mathrm{dt}} = -\mathrm{k_{dil}\,(cell_{(0)} + cell_{new})}$$

Additional equations:

$$\mathrm{k_{syn}} = \mathrm{k_{dec}(Hv_0 + lt_0)}$$

$$\mathrm{Half\,life} = \frac{0.693}{\mathrm{k_{dec}}}$$

Time 0 is defined as time when HM was changed to LM, Hv is the concentration of heavy peptide, lt is the concentration of light peptide, $cell_{new}$ is the number of new cells, k_{dec} is the first-order rate constant for degradation, k_{syn} is the zero-order rate constant for synthesis, k_{dil} is the first-order cell growth constant, $cell_{(0)}$ is the number of cells at time 0, $Hv_{(0)}$ is the concentration of heavy peptide at time 0, $lt_{(0)}$ is the concentration of light peptide at time 0. A step-wise approach was used for modeling wherein in the first step k_{dil} is estimated from the cell number and in the second step k_{dec} is estimated using above equations.

k_{dil} was estimated by quantifying the cell numbers after the change to LM and applying the following equation: A= $A_0 e^{-k_{dil}\, t}$ where A and A_0 represent the cell number at time t and 0, respectively.

Animal studies

All animal experimental protocols were approved by the Amgen Animal Care and Use Committee (AACUC) and were conducted in accordance with the guidelines set by the Association for Assessment and Accreditation of Laboratory Animal Care. The maximal tumor volume permitted by AACUC was 2500 mm^3, and this limit was not exceeded in any study. All studies utilized 4- to 7-week-old female athymic nude or female BALB/c mice (Charles River Laboratories). Mice were housed in an environmentally-controlled room (temperature 23 ± 2°C, relative humidity 50 ± 20%) on a 12-hour light/dark cycle. Mice were fed commercial rodent chow.

Tumor pharmacodynamic assays

The effect of AMG 510 on p-ERK was evaluated in MIA PaCa-2 T2, NCI-H358, and CT-26 *KRAS p.G12C* tumor-bearing mice. MIA PaCa-2 T2 or NCI-H358 tumor cells (5.0E+06 cells) were injected subcutaneously into the flank of female athymic nude mice in a mixture with Matrigel (BD Bioscience). Mice received a single oral dose of either vehicle or AMG 510 (0.3, 1, 3, 10, 30, and 100 mg/kg) when the average tumor size reached ~300-600 mm^3 (*n*=3/group) and harvested two hours later. A single dose of AMG 510 (10 mg/kg) was used for the time course studies. Female BALB/c mice were injected subcutaneously with CT-26 *KRAS p.G12C* tumor cells (3.0E+05 cells). Mice were randomized (*n*=3/group) when average tumor size reached ~500 mm^3 and received a single dose of either vehicle or AMG 510 (3, 10, 30,100 or 200 mg/kg), or MEKi (PD-

0325901, 10 mg/kg) and harvested two hours later. Tumor dimensions were collected with Pro-Max electronic digital caliper (Japan Micrometer Mfg. Co. LTD), and tumor volume was calculated using the formula: length x width x height and expressed as mm^3 using StudyDirector. For all studies, plasma and tumor were analyzed to determine test article concentrations. Tumor samples were collected at the indicated times and processed for bioanalysis or pulverized using a cryoPREP® Dry Impactor (Covaris). Pulverized samples were resuspended in RIPA lysis buffer containing protease and phosphatase inhibitors and homogenized. Cleared lysates were then assayed for p-ERK levels as described above and for covalent modification of $KRAS^{G12C}$ by MS. Data are expressed as mean ± SEM.

LC-MS/MS bioanalytical methods for AMG 510

Tumor tissue homogenates were prepared by adding water to tissue (4:1 mL:g) using tungsten carbide beads in a TissueLyzer (Qiagen). To 20 µL of sample (plasma or tumor tissue homogenate), 100 µL acetonitrile containing IS (200 ng/mL tolbutamide) was added, the sample was vortexed for 10 min, centrifuged at 3500 g for 10 min, and 90 µL of supernatant was collected. To the collected supernatant 100 µL of water (containing 0.1% formic acid) was added, and 5 µL of the resulting solution was injected onto the LC-MS/MS system. Chromatographic separations were achieved using a Phenomenex Kinetex C18 50 x 2.1 mm, 2.7 µm, maintained at 50°C, using 0.1% formic acid in H_2O (mobile phase A) and 0.1% formic acid in acetonitrile (mobile phase B). The chromatography gradient was run as follows: isocratic from 0 min to 0.1 min with 10% mobile phase B, linear increase from 0.1 to 0.85 min to 95% mobile phase B, isocratic hold from 0.85 to 1.10 min with 95% mobile phase B, linear decrease from 1.10 to 1.11

min to 10% mobile phase B, isocratic hold from 1.11 to 1.40 min with 10% mobile phase B. An API 4000 mass spectrometer was typically used for analysis and run in positive mode ESI following the MS/MS transition of 561.179 > 134.100 (AMG 510) and 271.100 > 134.100 (tolbutamide). Peak areas were integrated using Analyst® (Sciex). Following peak area integration, the data were exported to Watson LIMS™ (ThermoFisher Scientific) and concentrations were determined by a weighted ($1/x^2$) linear regression of peak area ratios (peak area of AMG 510/peak area of IS) versus the nominal concentrations of the plasma calibration standards. The calibration range for AMG 510 in plasma was 1.0 to 10,000 ng/mL (LLOQ 1.0 ng/mL). The calibration range for AMG 510 in tumor tissue homogenate was 5.0 to 50,000 ng/mL (LLOQ 5.0 ng/mL).

Xenograft and syngeneic studies

MIA PaCa-2 T2, NCI-H358, or SW480-1AC cells (5.0E+06 cells with Matrigel) were injected subcutaneously in the flank of female athymic nude mice (*n*=10/group). Treatment began when tumors were ~170 mm^3 for the MIA PaCa-2 T2 and NCI-H358 studies, or ~200 mm^3 for the SW480-1AC model. In the dose-response studies, mice received oral doses of either vehicle (QD) or AMG 510 (3, 10, 30, and 100 mg/kg QD). In the NCI-H358 combination study with AMG 510 and carboplatin, mice were randomized (*n*=10/group) and received either vehicle (QD) + PBS (1x/week); AMG 510 (10 or 30 mg/kg QD) + PBS (1x/week); vehicle (QD) + carboplatin (50 or 100 mg/kg) (1x/week); or AMG 510 orally (10 or 30 mg/kg QD) + carboplatin (50 or 100 mg/kg) (1x/week). For the combination study with AMG 510 and MEKi (PD-0325901), mice were randomized (*n*=10/group) and received either vehicle (QD); AMG 510 (10 mg/kg QD); MEKi (1 mg/kg QD); or AMG 510 (10 mg/kg QD) + MEKi (1 mg/kg QD).

For the syngeneic studies, CT-26 *KRAS p.G12C* cells (3.0E+05 cells) were injected subcutaneously in the flank of female BALB/c mice. Treatment began when tumors were ~170 mm^3 for the dose-response studies and ~130 mm^3 for the combination study (*n*=10/group), except the MEKi dose-response study (*n*=8/group). In the dose-response studies, mice received either vehicle (QD), AMG 510 (3, 10, 30, 100 or 200 mg/kg QD), or MEKi (1, 3, or 10 mg/kg QD). In the combination study, mice were randomized (*n*=10/group) on day 15 and received either vehicle (QD) + PBS (Q3Dx3); AMG 510 (100 mg/kg QD) + PBS (Q3Dx3); vehicle (QD) + anti-PD-1 antibody (29F.1A12; 100 µg/dose, Q3Dx3); or AMG 510 (100 mg/kg QD) + anti-PD-1 antibody (29F.1A12; 100 µg/dose, Q3Dx3) through day 43. Combination studies were blinded. CT-26 *KRAS p.G12C* cells (3.0E+05 cells) were injected subcutaneously in the flank of female BALB/c nude mice and received AMG 510 (200 mg/kg) from day 14 through day 32. Tumor dimensions were assessed twice weekly with Pro-Max electronic digital caliper (Japan Micrometer Mfg. Co. LTD), and tumor volume was calculated using the formula: length x width x height and expressed as mm^3 using StudyDirector. Data are expressed as mean ± SEM.

In the *KRAS p.G12C* lung and CRC PDX models, mice were implanted subcutaneously with tumor chunks (~70 mg). Mice were randomized when tumor volumes were ~160-200 mm^3 and received either vehicle (QD) or AMG 510 (100 mg/kg QD) after randomization. Tumor dimensions were calculated twice weekly using the formula: $width^2$ x length x 0.52 and expressed as mm^3 for NSCLC and SCLC models and width x length x height for the CRC PDX model. Data are expressed as mean ± SEM.

Flow cytometry

For *in vivo* studies, CT-26 *KRAS p.G12C* cells were implanted into ~6 week-old BALB/c female mice. On day 22 following implantation, mice were measured and randomized (*n*=8/group) as described above and received either vehicle (QD) + PBS (QDx1); AMG 510 (100 mg/kg QD) + PBS (QDx1); vehicle (QD) + anti-PD-1 antibody (29F.1A12; 100 µg/dose, QDx1); AMG 510 (100 mg/kg QD) + anti-PD-1 antibody (29F.1A12; 100 µg/dose, QDx1); or MEKi (PD-0325901; 10 mg/kg QD) + PBS (QDx1) for four days. After four days, tumors were harvested and placed in Liberase TL (0.2 mg/ml; Roche) and DNase I (20 µg/ml; Ambion). Tumor cell suspensions were then homogenized using a gentle MACS Dissociator (Miltenyi Biotech) and incubated at 37°C for 15 min on a MACSmix Tube Rotator (Miltenyi Biotech). Cells were then treated with 0.02% EDTA (Sigma) and heat-inactivated FBS (ThermoFisher Scientific) and filtered to remove clumps. After centrifugation, the cell pellets were resuspended in LIVE/DEAD Fixable Blue Dead Cell Stain (ThermoFisher Scientific) for 30 min. Cell surface staining was performed with the indicated antibodies (Supplementary Table 5) before fixation and permeabilization of the cells (Intracellular Fixation & Permeabilization Buffer Set, eBiosciences) for intracellular staining. CountBright™ Absolute Counting Beads (ThermoFisher Scientific) were added to each sample before analysis on an LSR II flow cytometer (BD Biosciences). All analyses were performed with FlowJo software v10 (FlowJo). Absolute cell counts were determined by normalizing cell numbers to beads recorded, divided by the volume of tumor aliquot analyzed and the mass of the tumor. Gating strategies are shown in Supplementary Fig. 2.

For *in vitro* analysis of the effect of AMG 510 on MHC Class I antigen expression, CT-26 *KRAS p.G12C* cells (5.0E+04 cells/well) were seeded in a 96-well plate and treated with a serial dilution of AMG 510 in the absence or presence of IFNγ at a final concentration of 25 or 250 pg/mL. Plates were incubated at 37°C, 5% CO_2 for 24 hours. Cells were non-enzymatically detached from the wells, washed with staining buffer (PBS/0.5% BSA), and then incubated with PE-conjugated H-2D^d, H-2K^d, or H-2L^d antibodies (BioLegend) for 30 min on ice. After washing, cells were resuspended in staining buffer containing SYTOX Blue Dead Cell Stain (Life Technologies), and then >1000 cells were analyzed by flow cytometry. Acquisition and analysis were performed on a BD LSRFortessa flow cytometer using BD FACSDiva software. Gating strategy is shown in Supplementary Fig. 3.

Enzyme-linked immunospot (ELISpot) assays

The antigen-specific T cell response was assessed using an IFN-γ ELISpot assay (Cellular Technology Ltd.). Splenocytes were harvested (*n*=4-5/group) and used in a whole-cell ELISpot assay. Briefly, 2.5E+05 splenocytes were mixed with 2.5E+04 CT-26, CT-26 *KRAS p.G12C*, or 4T1 tumor cells and incubated at 37°C for 20 hours. A CTLS6 Fluorospot analyzer (Cellular Technology Ltd.) was used to enumerate spots.

Gene expression analyses

Total RNA was purified by RNeasy Mini kits (QIAGEN) from CT-26 *KRAS p.G12C* tumors which were treated with oral doses of vehicle, AMG 510 (100 mg/kg QD), or MEKi (PD-0325901; 10 mg/kg QD) for two days (*n*=5/group). RNA was quantified by DropSense 96 (PerkinElmer Inc) and assayed on a nCounter™ (NanoString Technologies) with a mouse pan-cancer immune profiling panel containing 750 target genes, in addition to housekeeping genes and negative/positive controls. Raw data of individual genes were

quality controlled, normalized, and analyzed by nSolver v4.0 software (NanoString Technologies). Pathway scores (interferon score, antigen processing score, chemokine and receptors score, MHC score, TLR score, and T Cell function score) and cell profiling scores (NK cell score, cytotoxic cell score, and CD45 score) were generated by nSolver v4.0 (NanoString Technologies)[17].

See Supplementary Table 6 for genes included in each score, p values used to calculate pathway and cell profiling scores, and the statistical method (simplied negative binomial model or log-linear model) used by nSolver v4.0 to determine p values.

Immunohistochemistry

Routine immunohistochemical (IHC) assays directed against T cells (CD3, CD8), and proliferation (Ki67) markers were used to characterize cells in treated CT-26 *KRAS p.G12C* tumors. In brief, tumors were harvested after four days of treatment and fixed in 10% neutral-buffered formalin. After 48 hours of fixation, tumors were bisected and processed to paraffin blocks. Serial histologic sections were baked, deparaffinized in xylene, rehydrated with deionized water, and pretreated using Diva Heat-induced Epitope Retrieval buffers and the Decloaking Chamber NxGen (Biocare Medical). Endogenous proteins and peroxidases were blocked using Background Sniper (Biocare Medical) and PeroxiDAZED 1 (Biocare Medical). Histologic sections were incubated with the primary antibody or a species-matched IgG isotype control (Supplementary Table 3) for 1 h on an IntelliPATH™ Automated Staining System (Biocare Medical). The primary antibodies were detected using a horseradish peroxidase−labeled anti-rat (Biocare Medical) or anti-rabbit (Dako) IgG for 30 min followed by 3,3-diaminobenzidine (DAB) chromogen substrate (Dako), and counter-stained with hematoxylin (Dako). For the CD3/Ki67 dual

IHC assay, there were two antibody-complex incubation cycles separated by a reagent-based Denaturation Solution step (Biocare Medical). The CD3-complex was visualized with DAB, the Ki67-complex was visualized with 3,3',5,5'-tetramethylbenzidine (Vector Labs), and the nuclei were counterstained with Nuclear Fast Red (Vector Labs). Slides were dehydrated in 100% ethanol, cleared in xylene, and coverslipped. Light microscopic analysis of histologic sections was performed using a Nikon Eclipse 90i. Appropriate immunostain patterns for each IHC assay and isotype control was confirmed using lymph nodes harvested with the tumors (internal control tissue).

Dendritic cell and T cell co-cultures

Mouse bone marrow cells were cultured for 6 days in the presence of recombinant mouse GM-CSF to generate bone marrow-derived dendritic cells (BMDCs). BMDCs were then pulsed overnight with 50 µg/mL ova protein with or without AMG 510 or MEKi at IC_{90} concentrations. Alternatively, BMDCs were pulsed with SIINFEKL peptide as a positive control or were not antigen-pulsed as a negative control. The next day, CD8+ T cells were enriched from spleens of OT-I transgenic mice by magnetic separation and labeled with CellTrace Violet (CTV; Invitrogen). Pulsed BMDCs were washed to remove excess ova protein and small molecule inhibitors. For co-cultures, 1.0E+05 T cells were combined with 5.0E+03 BMDCs in 96-well plates with or without further AMG 510 or MEKi. Co-cultures were incubated for three days at 37°C. Cell division was assessed by flow cytometry by measuring CTV dilution in $TCR\beta^+$ $CD8\alpha^+$ cells. Gating strategy is shown in Supplementary Fig. 4.

CXCL10 / CXCL11 transcript and IP-10 protein analysis

Parental CT-26 or CT-26 *KRAS p.G12C* cells were seeded in 6-well plates at a density of 5.0E+05 cells/well (*n*=4 replicates) and incubated at 37°C, 5% CO_2 for 16 h. Cells were treated with 0.1% DMSO, 5 µM AMG 510, or 0.02 µM MEKi (2 h basal p-ERK IC_{90}). Following incubation at 37°C, 5% CO_2 for 24 h, conditioned media were collected from each well and used for quantification of IP-10 protein according to the kit manufacturer's protocol (Meso Scale Discovery). The adherent cells were washed with PBS, and RNA was prepared for gene expression analysis by Nanostring as described previously in the Methods section.

Clinical trial NCT03600883

This study was conducted in compliance with all relevant ethical regulations. The protocol, proposed informed consent form, other written subject information, and any proposed advertising material were submitted to the institutional review boards (IRB)/independent ethics committees (IEC) of all clinical study sites for written approval. The investigator submitted and, where necessary, obtained approval from the IRB/IEC for all subsequent protocol amendments and changes to the informed consent document. The investigator notified the IRB/IEC of deviations from the protocol or serious adverse events occurring at the site and other adverse event reports received from Amgen, in accordance with local procedures. The investigator was responsible for obtaining annual IRB/IEC approval/renewal throughout the duration of the study. Copies of the investigator's reports and the IRB/IEC continuance of approval were sent to Amgen.

Before a subject's participation in the clinical study, the investigator was responsible for obtaining written informed consent from the subject or legally acceptable representative

after adequate explanation of the aims, methods, anticipated benefits, and potential hazards of the study and before any protocol-specific screening procedures or any investigational product(s) were administered. A copy of the written approval of the protocol and informed consent form was received by Amgen before recruitment of subjects into the study and shipment of Amgen investigational product.

Statistics and reproducibility

In vitro experiments were repeated the indicated number of times with similar results, except for immunoblot data which are from a single experiment. Kinetic properties (k_{obs}, K_I, and $[I]_{50}$) and standard error were determined from nonlinear curve fitting of experimental values (see Source Data for Fig. 1c and Extended Data Fig. 1e, f for *n*). Synergy scores were determined from the aggregrate of two 10x10 matrices for adherent monolayer combinations, but a single 6x10 matrix for spheroid combinations. Data for the cell surface expression of MHC class I antigens reported in Fig. 5e and Extended Data Fig. 10c are representative of *n*=2 experiments. Data reported for *in vivo* studies were each from a single experiment, except for the data presented in Fig. 2g, Fig. 4d, e; Extended Data Fig. 3a, b; and Extended Data Fig. 10d, which were repeated twice with similar results.

Pharmacodynamic experiments were analyzed by two-sided, one-way ANOVA followed by Dunnett's post-hoc multiple comparison test using the Biostatistical Analysis R Shiny application (Shiny v1.0.5). For efficacy studies, two-sided repeated measures analysis of variance (RM ANOVA) was conducted followed by Dunnett's post-hoc test multiple comparison test using Prism (GraphPad Software v7.04). Regression analysis was conducted by two-sided t-test. Statistical analysis for survival was determined by two-

sided Kaplan-Meier estimator with Mantel-Cox log-rank to compare curves using Prism. Flow cytometry, NanoString, and T-cell proliferation data were analyzed by two-sided, one-way ANOVA followed by Tukey's multiple comparison post-hoc test using Prism. ELISpot data comparisons were performed by two-sided t-test using Prism. Comparison of CXCL10 and CXCL11 transcript levels and secreted IP-10 protein levels were performed by two-sided, two-way ANOVA followed by Tukey's multiple comparison post-hoc test.

Supplementary Table 1. Cellular assay data

Mutation	Cell Line	Tissue of Origin	Basal pERK1/2 Mean IC_{50} (μM)	Cell Viability Mean IC_{50} (μM)	Spheroid Cell Viability Mean IC_{50} (μM)
KRAS p.G12C homozygous	MIA PaCa-2 ATCC® CRL-1420™	Pancreas	0.033 ± 0.004 *n*=6	0.005 ± 0.001 *n*=67	0.001 ± 0.0004 *n*=4
	NCI-H1373 ATCC® CRL-5866™	Lung	0.010 *n*=2	0.021 ± 0.008 *n*=3	0.005 ± 0.002 *n*=6
	NCI-H2030 ATCC® CRL-5914™	Lung	0.040 *n*=2	0.006 ± 0.003 *n*=3	ND
	NCI-H2122 ATCC® CRL-5985™	Lung	0.123 *n*=2	0.032 *n*=2	0.009 ± 0.002 *n*=4
	SW1463 ATCC® CCL-234™	Colon	0.033 ± 0.004 *n*=3	0.015 ± 0.007 *n*=4	ND
	SW1573 ATCC® CRL-2170™	Lung	0.027 *n*=2	> 7.5 *n*=2	>10 *n*=5
	UM-UC-3 ATCC® CRL-1749™	Bladder	0.029 *n*=2	0.005 *n*=2	ND
KRAS p.G12C heterozygous	Calu-1 ATCC® HTB-54™	Lung	0.013 *n*=2	0.004 *n*=2	ND
	NCI-H1792 ATCC® CRL-5895™	Lung	0.045 *n*=2	0.011 *n*=2	ND
	NCI-H23 ATCC® CRL-5800™	Lung	0.090 *n*=2	0.006 *n*=2	ND
	NCI-H358 ATCC® CRL-5807™	Lung	0.027 ± 0.011 *n*=5	0.004 ± 0.001 *n*=3	0.003 ± 0.002 *n*=6
	SW837 ATCC® CCL-235™	Colon	0.018 ± 0.002 *n*=3	0.009 ± 0.006 *n*=4	ND
KRAS p.G12D homozygous	AsPC-1 ATCC® CRL-1682™	Pancreas	> 10 *n*=3	> 7.5 *n*=3	ND
KRAS p.G12D heterozygous	A-427 ATCC® HTB-53™	Lung	> 10 *n*=2	> 7.5 *n*=2	ND
	LS 174T ATCC® CL-188™	Colon	> 10 *n*=1	> 7.5 *n*=1	ND

Mutation	Cell Line	Tissue of Origin	Basal pERK1/2 Mean IC_{50} (µM)	Cell Viability Mean IC_{50} (µM)	Spheroid Cell Viability Mean IC_{50} (µM)
KRAS p.G12V homozygous	SW480 ATCC® CCL-228™	Colon	> 10 *n*=2	> 7.5 *n*=2	ND
KRAS p.G12S homozygous	A549 ATCC® CCL-185™	Lung	> 10 *n*=3	> 7.5 *n*=40	ND
KRAS p.G13C heterozygous	NCI-H1355 ATCC® CRL-5865™	Lung	> 10 *n*=2	> 7.5 *n*=2	ND
KRAS WT *EGFR p.E746_A750del*	HCC-827 ATCC® CRL-2868™	Lung	> 10 *n*=3	> 7.5 *n*=2	ND
KRAS WT *EML4-ALK* fusion	NCI-H1322 NCI	Lung	> 10 *n*=2	> 7.5 *n*=2	ND
KRAS WT *TPM3-NTRK* fusion	KM12 NCI	Colon	> 10 *n*=2	> 7.5 *n*=2	ND
KRAS WT *BRAF p.V600E*	COLO-205 ATCC® CCL-222™	Colon	> 10 *n*=2	> 7.5 *n*=2	ND

ATCC, American Type Culture Collection; NCI, National Cancer Institute; ND, not determined.

Mutation annotations were obtained from the Catalogue of Somatic Mutations in Cancer (COSMIC)[18] or Misale et al. 2019[19]. Mean IC_{50} values and SD for basal ERK1/2 phosphorylation and cell viability assays were obtained from the number of experiments indicated.

Supplementary Table 2. NCI-H358 cysteine proteome analysis

Identification and quantitation of desthiobiotinylated peptides was obtained using database searching via a custom informatics pipeline developed in the Gygi Lab at Harvard Medical School that utilizes SEQUEST[20]. Database search parameters are included in Supplementary Table 2. Log_2 fold changes were calculated between DMSO control and AMG 510-treated sample groups (*n*=5/group), and a two-tailed t test for each peptide was performed to assess the statistical significance of difference between treated and DMSO control sample groups assuming equal variance.

Supplementary Table 3. AMG 510 combination matrices and synergy scores

Cell Line	Inhibitor combination	Synergy score		Max [inhibitor] (μM)
		Combination	Self-cross	
NCI-H358	afatinib AMG 510	21.3	0.253 0.662	1 (1:2.5) 0.2 (1:3)
	erlotinib AMG 510	12.4	0.547 1.36	5 (1:2) 0.3 (1:3)
	RMC-4550 AMG 510	22.8	0.458 1.89	10 (1:3) 0.067 (1:3)
	trametinib AMG 510	14.7	1.21 1.63	0.3 (1:3) 0.1 (1:3)
	AMG 511 AMG 510	7.41	0.526 1.89	1 (1:2) 0.067 (1:3)
	AZD5363 AMG 510	3.16	0.069 1.63	10 (1:2) 0.1 (1:3)
MIA PaCa-2	afatinib AMG 510	4.19	2.08 0.897	5 (1:2) 0.2 (1:3)
	erlotinib AMG 510	2.07	0.357 0.897	10 (1:2) 0.2 (1:3)
	RMC-4550 AMG 510	6.36	0.242 0.897	10 (1:2) 0.2 (1:3)
	trametinib AMG 510	3.06	ND 0.897	0.2 (1:3) 0.2 (1:3)
	AMG 511 AMG 510	5.53	0.193 0.897	1 (1:2) 0.2 (1:3)
	AZD5363 AMG 510	2.67	0.128 0.897	10 (1:2) 0.2 (1:3)
NCI-H1373	afatinib AMG 510	9.59	1.14 1.31	2.5 (1:2) 5 (1:3)
	RMC-4550 AMG 510	5.96	0.315 1.31	10 (1:2.5) 5 (1:3)
	trametinib AMG 510	5.97	0.245 1.31	1 (1:3) 5 (1:3)
	AMG 511 AMG 510	11.8	0.355 1.31	1 (1:3) 5 (1:3)
SW1573	RMC-4550 AMG 510	2.15	0.107 0.140	10 (1:3) 10 (1:3)
	trametinib AMG 510	0.817	0.141 0.140	0.5 (1:2) 10 (1:3)
	AMG 511 AMG 510	3.87	0.782 0.140	3 (1:3) 10 (1:3)

Cell Line	Inhibitor combination	Synergy score		Max [inhibitor] (μM)
		Combination	Self-cross	
MIA PaCa-2 spheroid	afatinib AMG 510	1.5	2.08 1.33	2.5 (1:2) 0.05 (1:4)
	trametinib AMG 510	8.31	4.14 1.33	0.1 (1:3) 0.05 (1:4)
NCI-H1373 spheroid	afatinib AMG 510	8.7	0.931 1.24	2.5 (1:2) 0.05 (1:4)
	trametinib AMG 510	11.8	3.76 1.24	1 (1:3) 0.05 (1:4)
CT-26 *KRAS p.G12C* spheroid	afatinib AMG 510	10.8	1.37 1.47	5 (1:2.5) 0.25 (1:4)
	RMC-4550 AMG 510	11.7	4.14 1.47	5 (1:2.5) 0.25 (1:4)
	trametinib AMG 510	2.63	2.21 1.47	0.01 (1:2.5) 0.25 (1:4)
	AMG 511 AMG 510	10.8	2.24 1.47	0.5 (1:2.5) 0.25 (1:4)

Synergy scores and maximum concentration tested of the inhibitors and the dose titration range covered by the matrices in each combination are listed. Individual heterologous combinations (A x B) were evaluated by comparing their respective synergy scores to that of their component self-crosses (A x A or B x B). Heterologous combinations were considered synergistic only when their synergy score exceeded three times that of either component self-cross synergy score.

Supplementary Table 4. Chemokine / receptor gene expression in CT-26 *KRAS p.G12C* tumors following AMG 510 treatment

Gene	Fold Change (AMG 510 / Vehicle)
CCL8	3.51
CXCR6	3.35
CCR3	2.89
CCL28	2.75
XCR1	2.66
XCL1	2.63
IL16	2.53
CCL5	2.49
CX3CR1	2.44
CCL1	2.34
CMKLR1	2.31
CCL24	2.28
CCR2	2.22
IL6RA	2.19
CXCR4	1.93
CXCL11	1.76
CXCL9	1.76
CXCL16	1.47
CCR5	1.41

RNA was isolated from CT-26 *KRAS p.G12C* tumors after two days of treatment. Changes in gene expression were calculated by NanoString technology (*n*=5/group). Chemokine / receptor genes which were induced by AMG 510 treatment (>1.4-fold) are shown.

Supplementary Table 5. Antibodies for immunoblotting, immunohistochemistry, and flow cytometry

Antibody	Clone	Catalog #	Supplier	Lot #	Antibody Dilution
Rabbit anti-phospho-EGF Receptor (Tyr1068)	D7A5	3777	Cell Signaling	13	1:1,000 (IB)
Rabbit anti-EGF Receptor	D38B1	4267	Cell Signaling	11	1:1,000 (IB)
Rabbit anti-Phospho-MEK1/2 (Ser217/221)	-	9121	Cell Signaling	44	1:1,000 (IB)
Rabbit anti-MEK1/2	-	9122	Cell Signaling	14	1:1,000 (IB)
Rabbit anti-phospho-S6 Ribosomal Protein (Ser235/236)	D57.2.2E	4858	Cell Signaling	16	1:1,000 (IB)
Rabbit anti-S6 Ribosomal Protein	5G10	2217	Cell Signaling	7	1:1,000 (IB)
Rabbit anti-phospho-Akt (Ser473)	D9E	4060	Cell Signaling	19	1:1,000 (IB)
Rabbit anti-Akt	-	9272	Cell Signaling	27	1:1,000 (IB)
Rabbit anti-phospho-ERK1/ERK2 (Thr185, Tyr187)	-	44-680G	ThermoFisher Scientific	SB248818	1:1,000 (IB)
Rabbit anti-p44/42 MAPK (Erk1/2)	-	9102	Cell Signaling	26	1:1,000 (IB)
Rabbit anti-Ras	EPR3255	ab108602	Abcam	GR117071-23	1:1,000 (IB)
Rabbit anti-cleaved Caspase-3 (Asp175)	-	9661	Cell Signaling	45	1:1,000 (IB) 1:400 (IHC)
Mouse anti-β-actin-peroxidase	AC-15	A3854	Sigma	026M4820V	1:20,000 (IB)
Donkey anti-rabbit IgG-HRP	-	NA934V	GE Healthcare	9677977	1:5,000 (IB)
Rat anti-human CD3 (mouse CD3 cross-reactive)	CD3-12	MCA1477	Bio-Rad	7708	1:1,000 (IHC)
BUV737 Rat Anti-Mouse CD4	RM4-5	564933	BD Biosciences	8164630	1:100 (FC)
BV421 Rat Anti-Mouse CD8a	53-6.7	563898	BD Biosciences	7201962	1:100 (FC)
Rabbit Anti-Mouse CD8a	D4W2Z	98941	Cell Signaling Technology	0712017	1:500 (IHC)
APC Rat Anti-Mouse CD8a	53-6.7	17-0081-82	eBioscience	E07056-1635	1:100 (FC)
BUV737 Rat Anti-CD11b	M1/70	564443	BD Biosciences	7338572	1:100 (FC)

Antibody	Clone	Catalog #	Supplier	Lot #	Antibody Dilution
Rat Anti-Mouse CD16/CD32	2.4G2	553142	BD Biosciences	4198965	1:100 (FC)
FITC Rat Anti-Mouse CD24	M1/69	11-0242-81	ThermoFisher Scientific	1937898	1:100 (FC)
BV786 Mouse Anti-Mouse CD45.2	104	563686	BD Biosciences	8235903	1:100 (FC)
APC/Cy7 Rat Anti-Mouse CD90.2	30-H12	105328	BioLegend	B241601	1:100 (FC)
APC Hamster Anti-Mouse CD103	2E7	17-1031-80	ThermoFisher Scientific	4322558	1:100 (FC)
PE Hamster Anti-Mouse CD279 (PD-1)	J43	12-9985-82	ThermoFisher Scientific	4329622	1:100 (FC)
BV650 Rat Anti-Mouse F4/80	BM8	123149	BioLegend	B256505	1:100 (FC)
PE Mouse anti-mouse H-2D^{d}	34-2-12	110608	Biolegend	B256526	1:100 (FC)
PE Mouse anti-mouse H-2K^{d}	SF1-1.1	116608	Biolegend	B244820	1:100 (FC)
PE Mouse anti-mouse H-2L^{d}/H-2D^{b}	28-14-8	114507	Biolegend	B240332	1:100 (FC)
Rabbit anti-human Ki67 (mouse Ki67 cross-reactive)	SP6	275R-1	Sigma-Aldrich	45305	1:500 (IHC)
BV711 Rat Anti-Mouse Ly-6C	HK1.4	128037	BioLegend	B247973	1:1,000 (FC)
APC-H7 Rat Anti-Mouse Ly-6G	1A8	565369	BD Biosciences	8121728	1:100 (FC)
BV510 Rat Anti-Mouse I-A/I-E (MHCII)	M5/114.15.2	107635	BioLegend	B263357	1:500 (FC)
BV711 Hamster Anti-Mouse TCR β Chain	H57-597	563135	BD Biosciences	7054698	1:100 (FC)
FITC Hamster Anti-Mouse TCR β Chain	H57-597	553171	BD Biosciences	8351664	1:100 (FC)
7-AAD	-	559925	BD Biosciences	82639992	1:100 (FC)
Rat IgG Isotype Negative Control	-	012-000-003	Jackson Immunoresearch Labs	68714	2 µg/mL (IHC)
Rabbit IgG Isotype Negative Control	-	011-000-003	Jackson Immunoresearch Labs	132409	2 µg/mL (IHC)
HRP-anti-rat IgG	-	BRR4016L	Biocare Medical	100317	none (IHC)
HRP-anti-rabbit IgG	-	K4003	Dako	10147964	none (IHC)

IB, immunoblot; IHC, immunohistochemistry; FC, flow cytometry

Supplementary Table 6. Gene expression pathway score analysis

Pathway scores (interferon score, antigen processing score, chemokine and receptors score, MHC score, TLR score, and T Cell function score) and cell profiling scores (NK cell score, cytotoxic cell score, and CD45 score) were generated by nSolver v4.0 (NanoString Technologies)[17]. The genes included in each score, p values used to calculate pathway and cell profiling scores, and the statistical method used by nSolver v4.0 to determine p values are listed in Supplementary Table 6. lm.nb, simplified negative binomal model; loglinear, log-linear model.

Supplementary Figure 1a

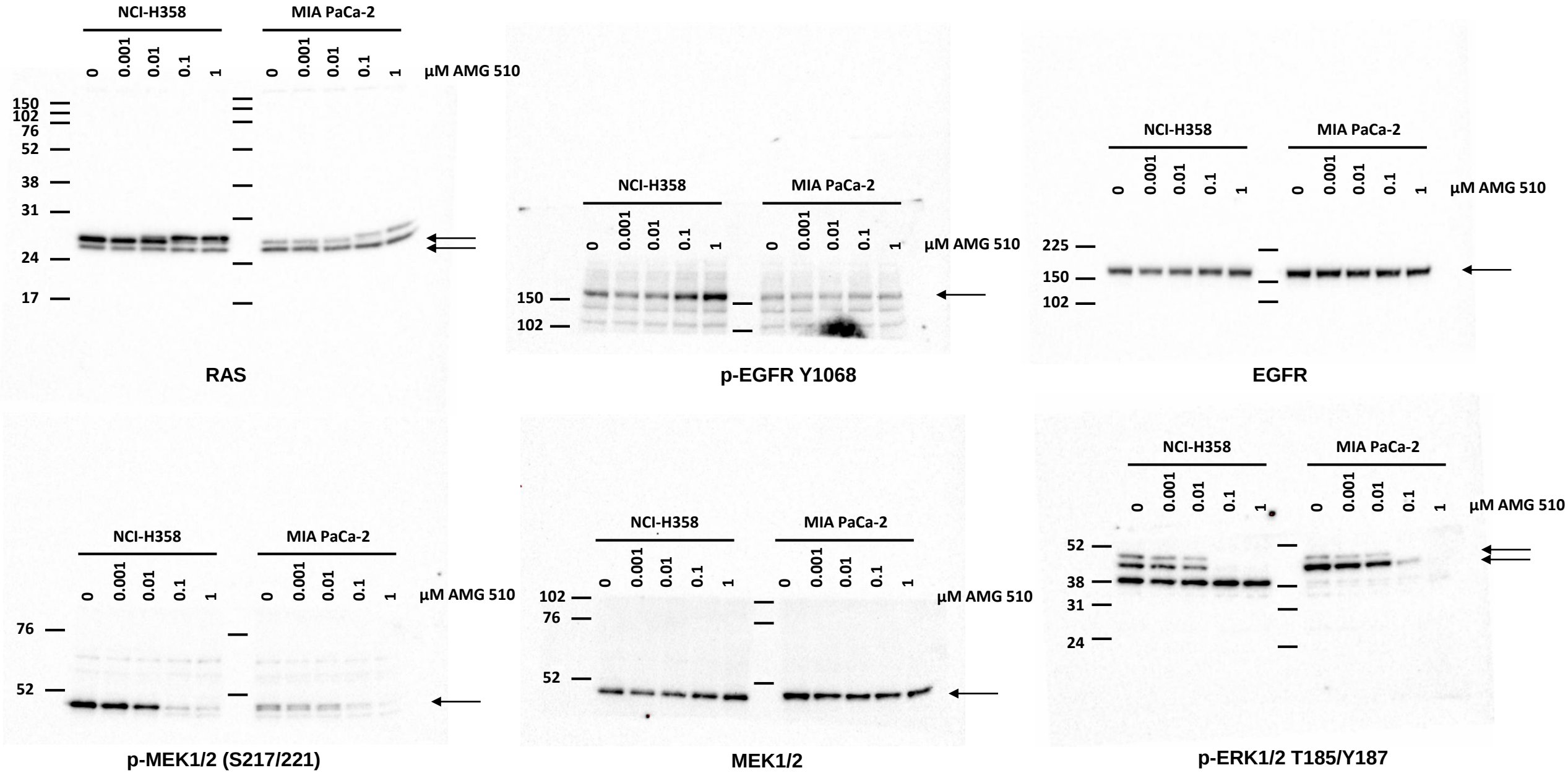

Supplementary Figure 1a (cont'd)

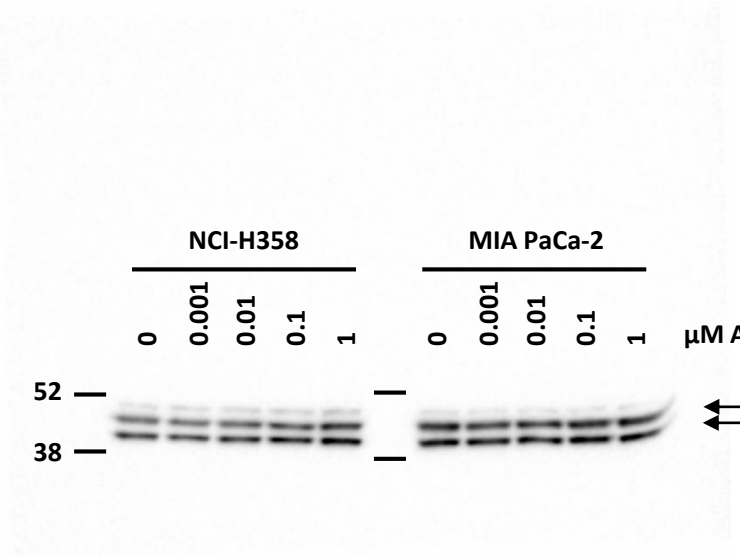

ERK1/2

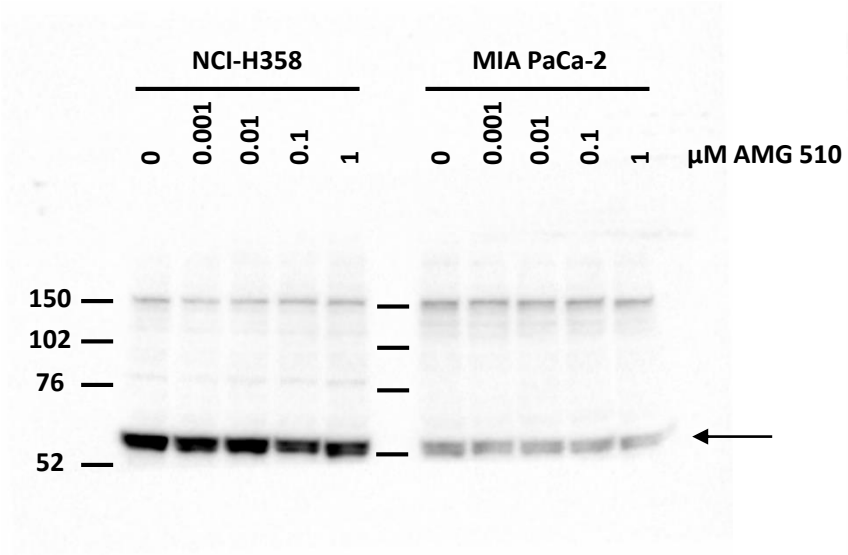

p-AKT S473

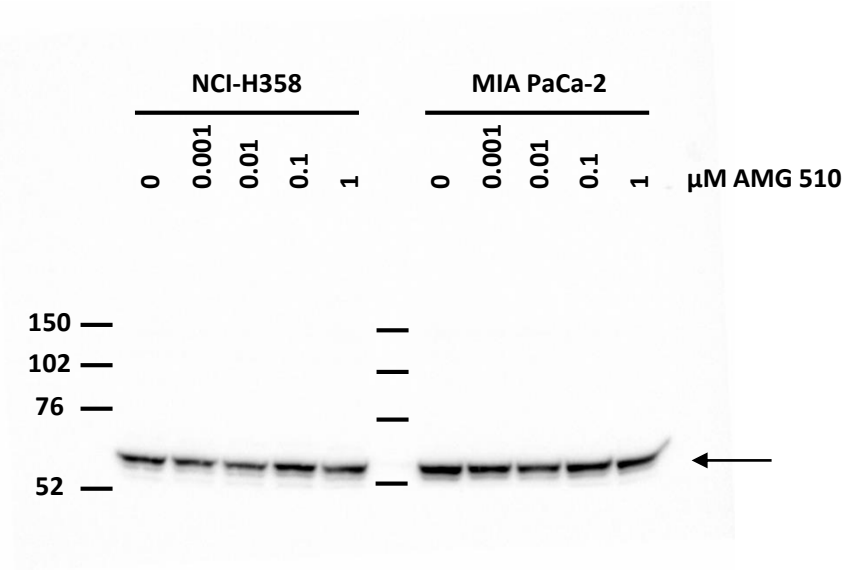

AKT

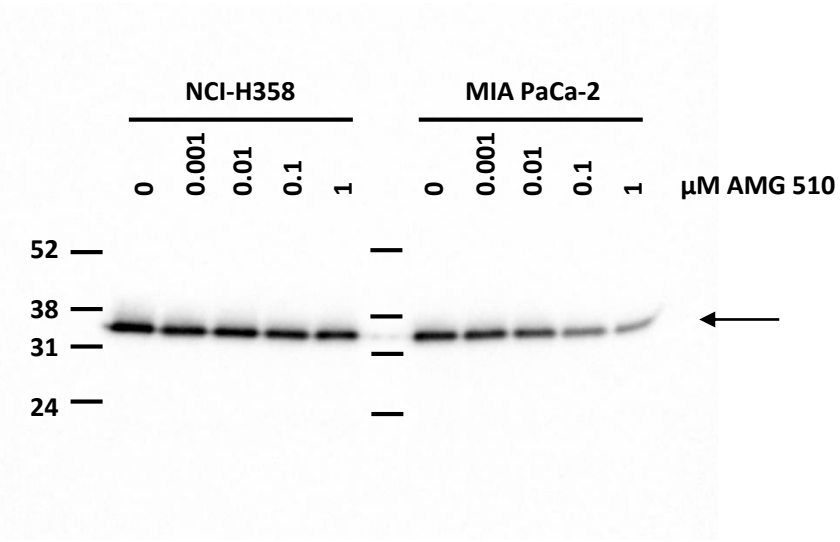

p-S6 S235/236

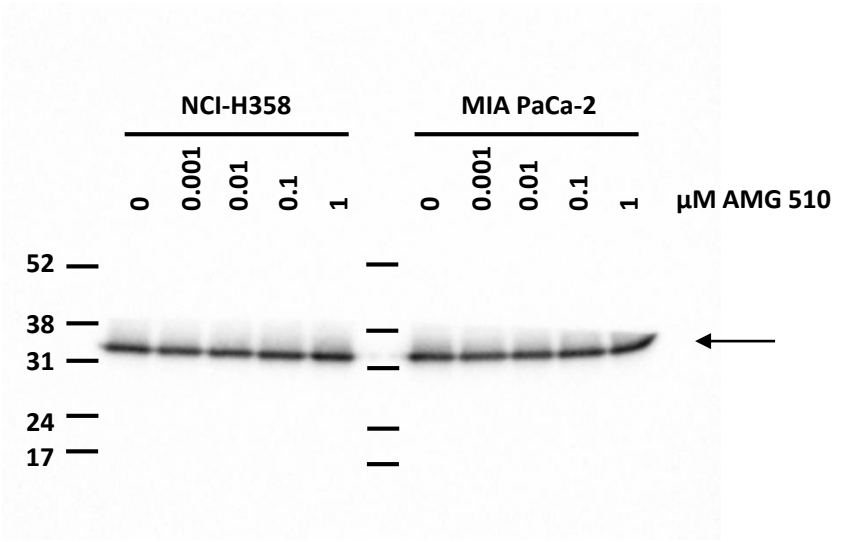

S6

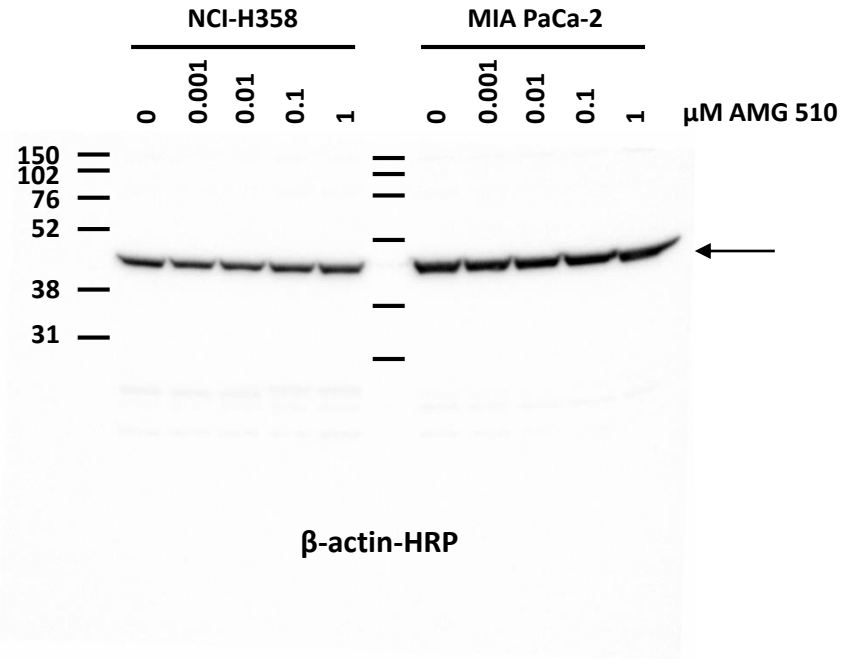

β-actin-HRP

Supplementary Figure 1b

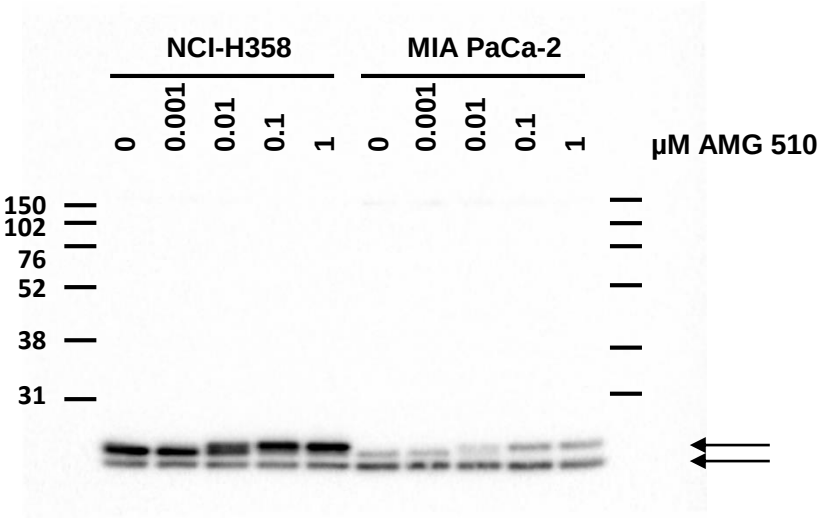

RAS

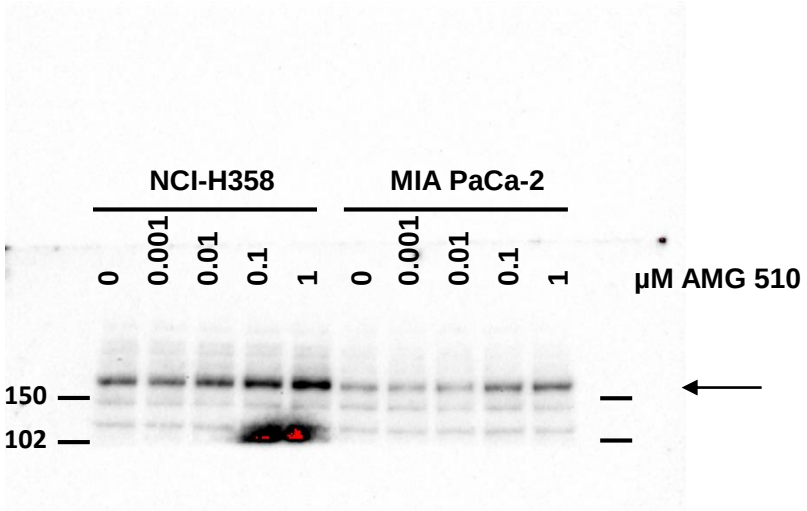

p-EGFR Y1068

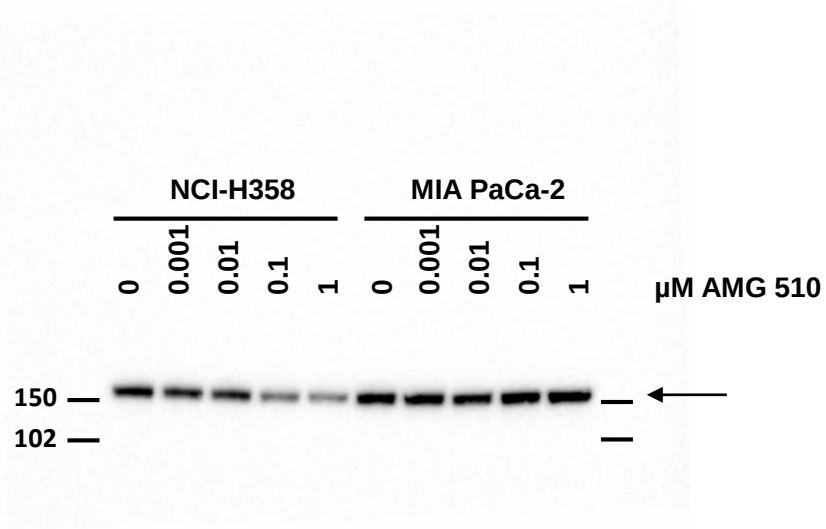

EGFR

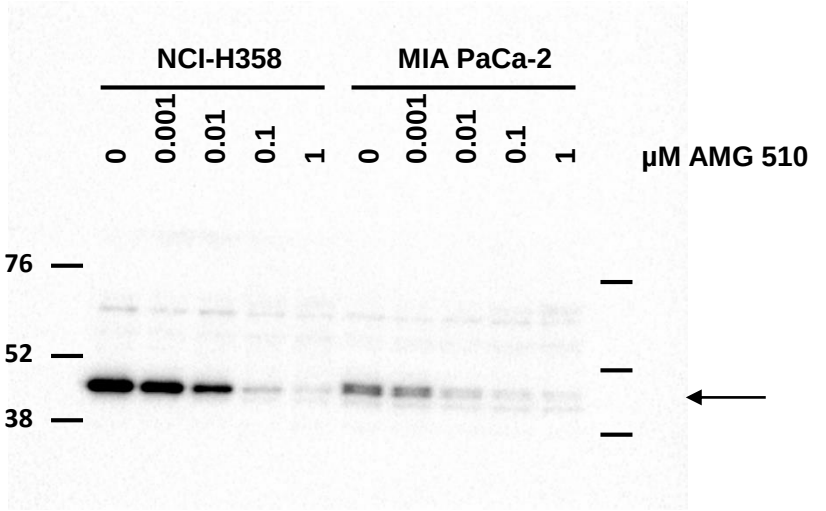

p-MEK1/2 (S217/221)

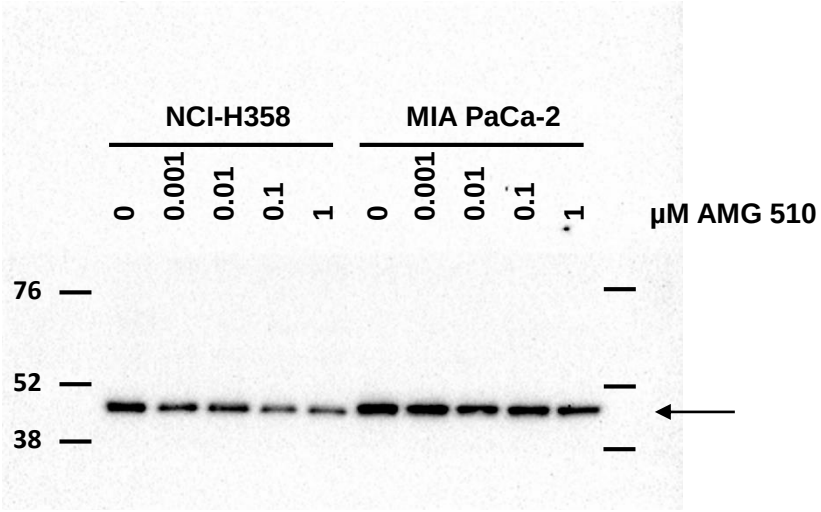

MEK1/2

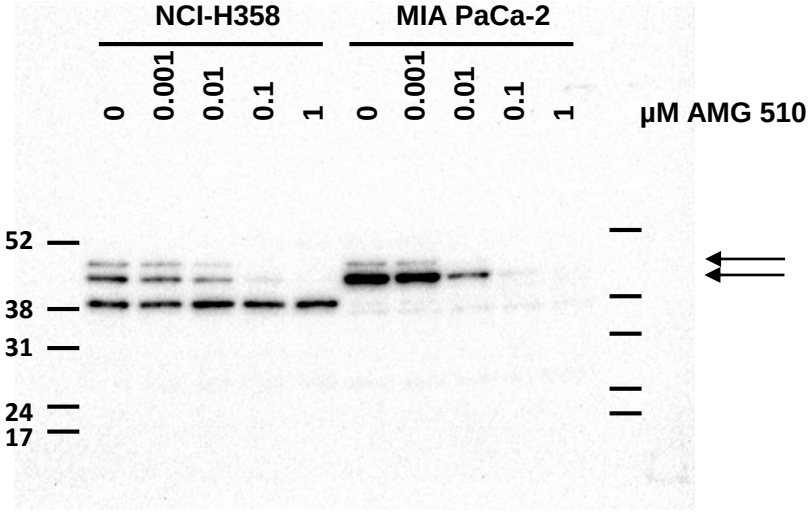

p-ERK1/2 T185/Y187

Supplementary Figure 1b (cont'd)

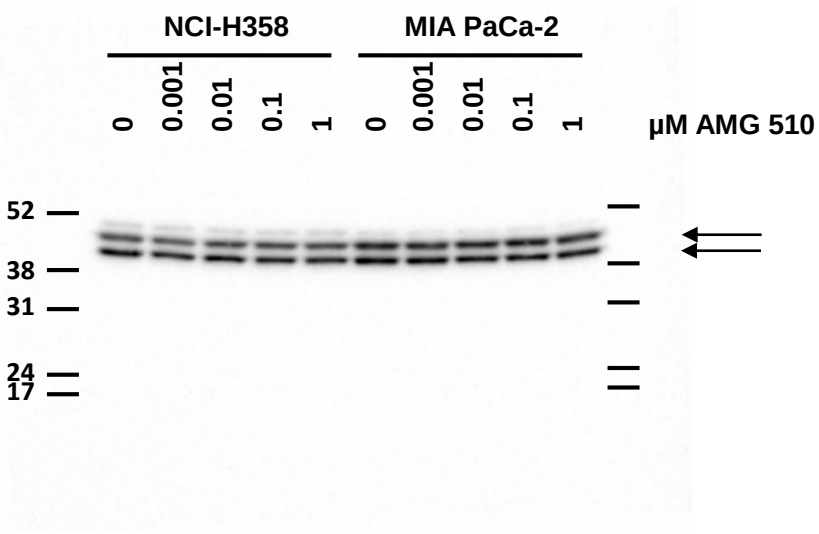

ERK1/2

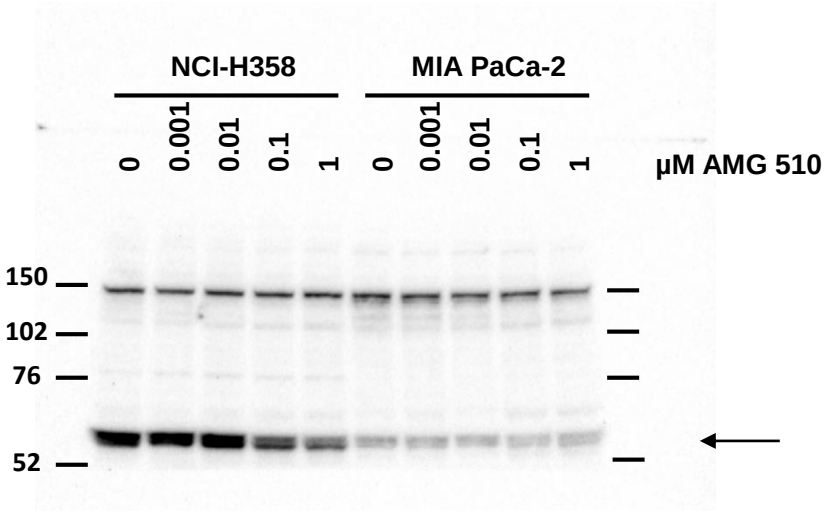

p-AKT S473

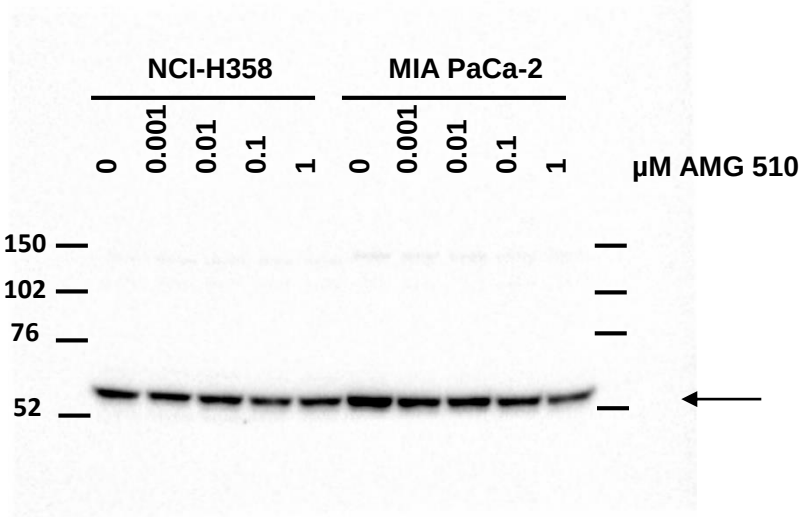

AKT

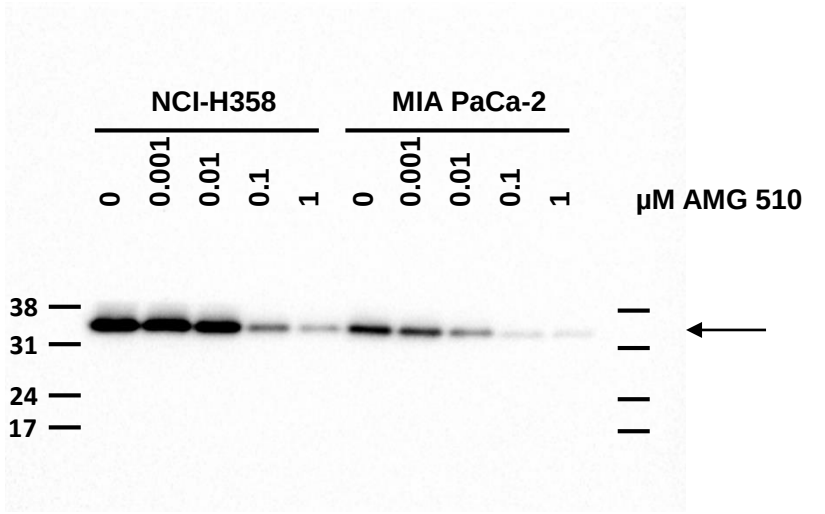

p-S6 S235/236

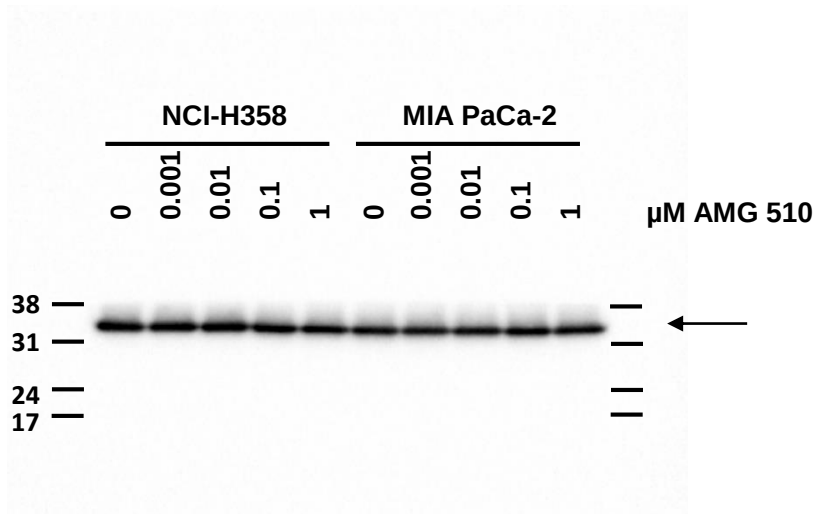

S6

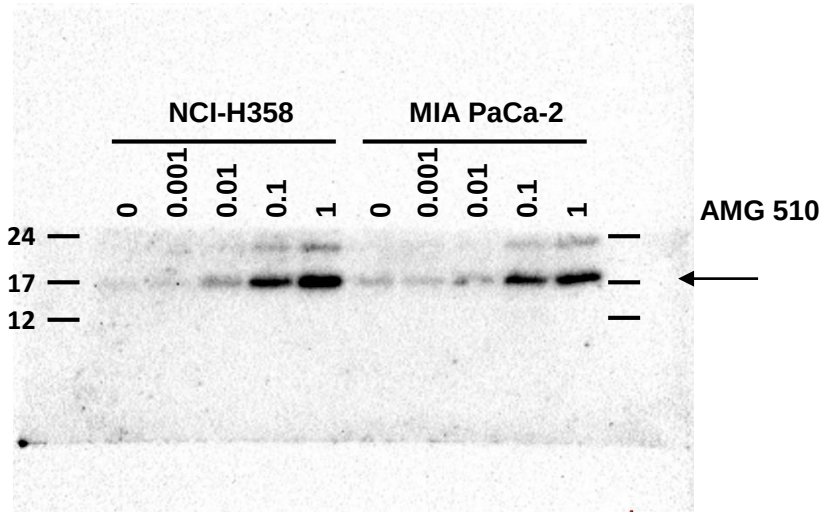

cleaved caspase-3

Supplementary Figure 1b (cont'd)

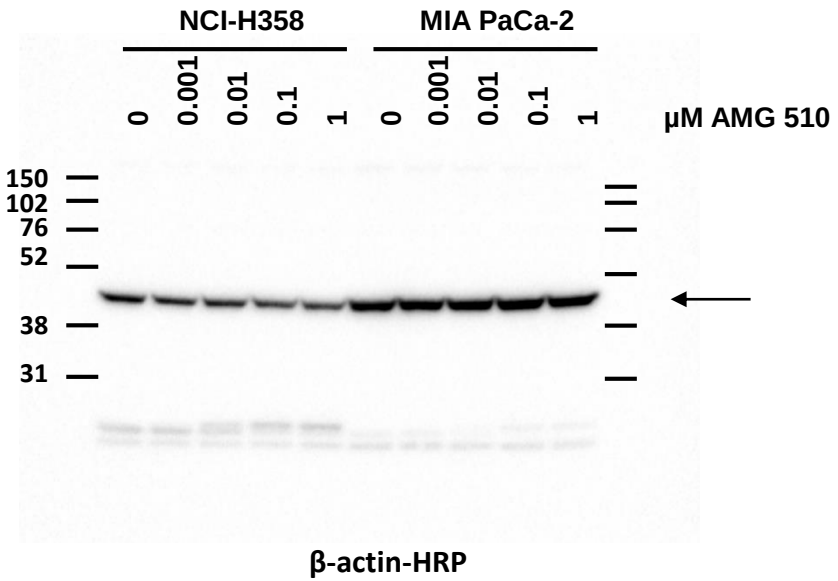

Supplementary Figure 1c

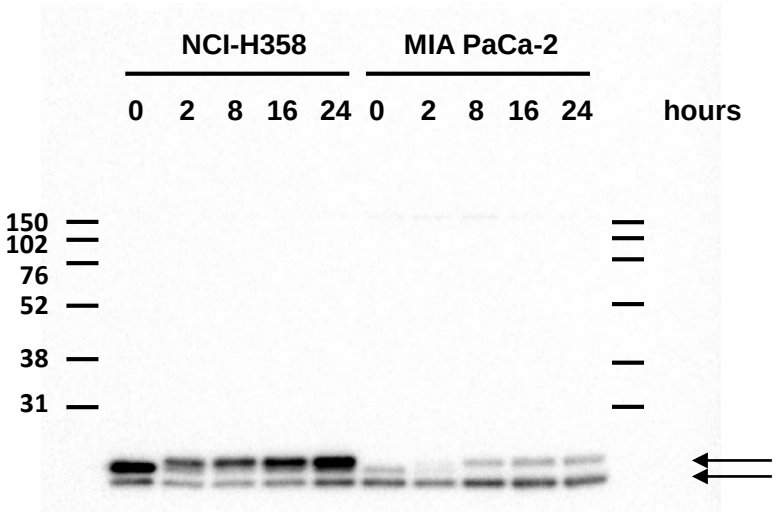

RAS

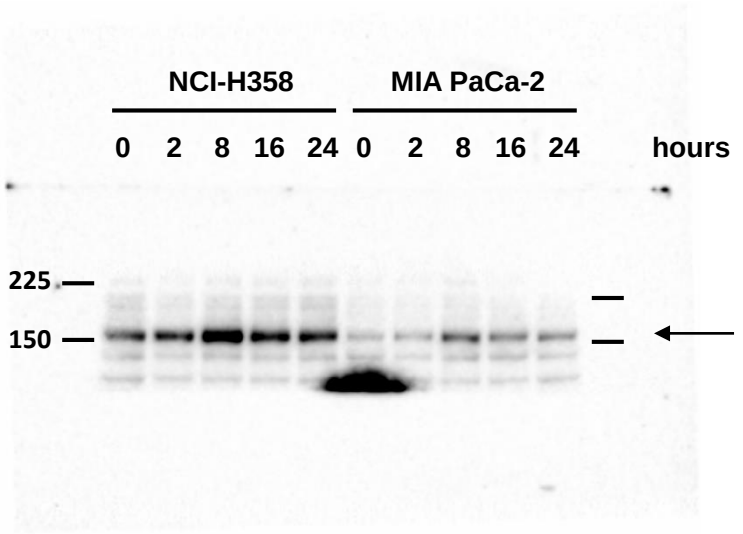

p-EGFR Y1068

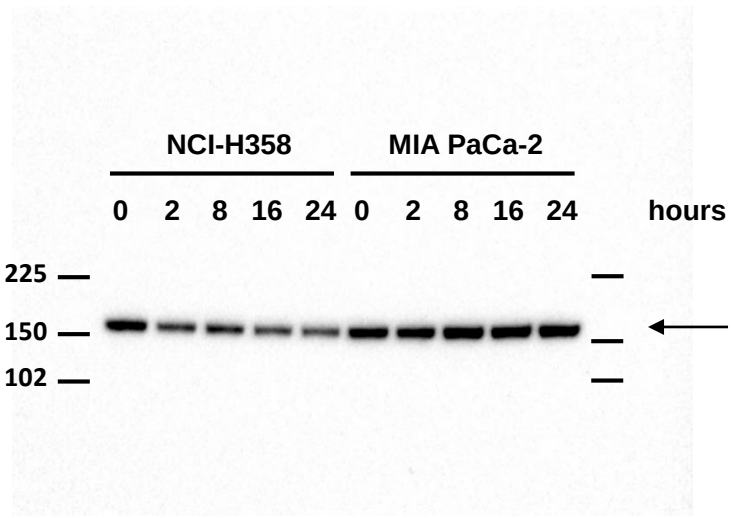

EGFR

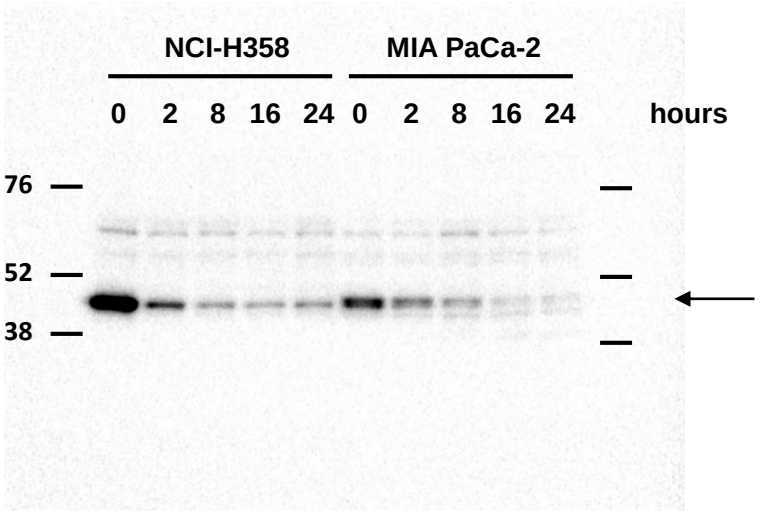

p-MEK1/2 (S217/221)

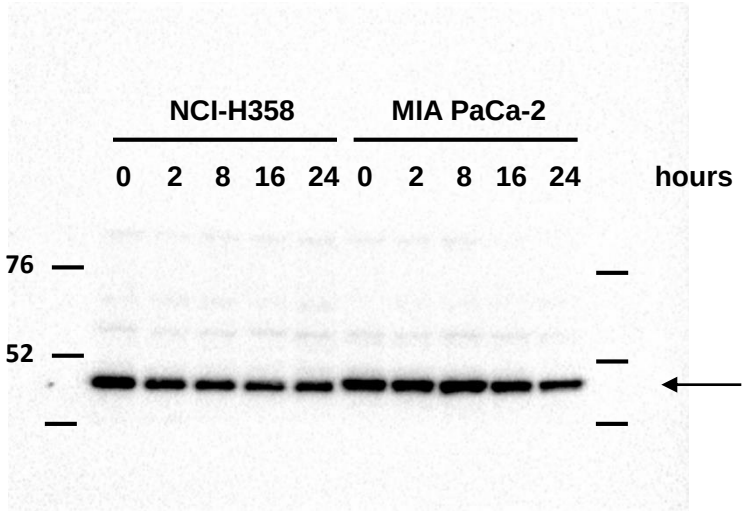

MEK1/2

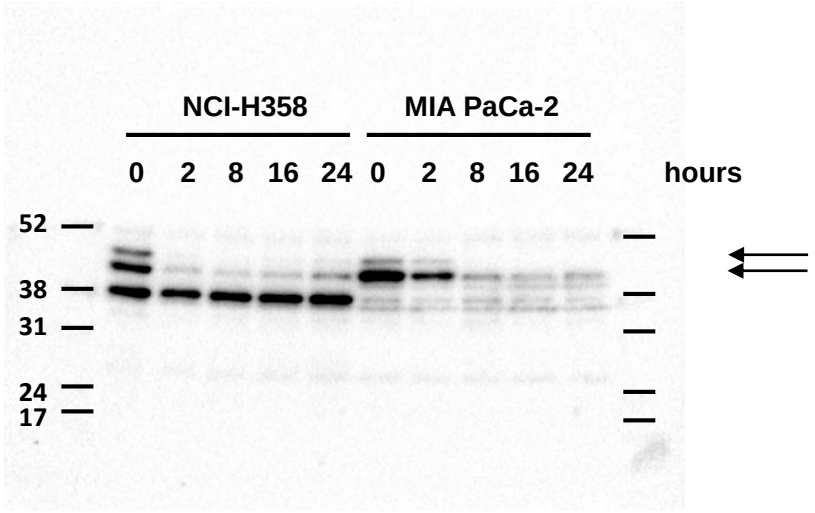

p-ERK1/2 T185/Y187

Supplementary Figure 1c (cont'd)

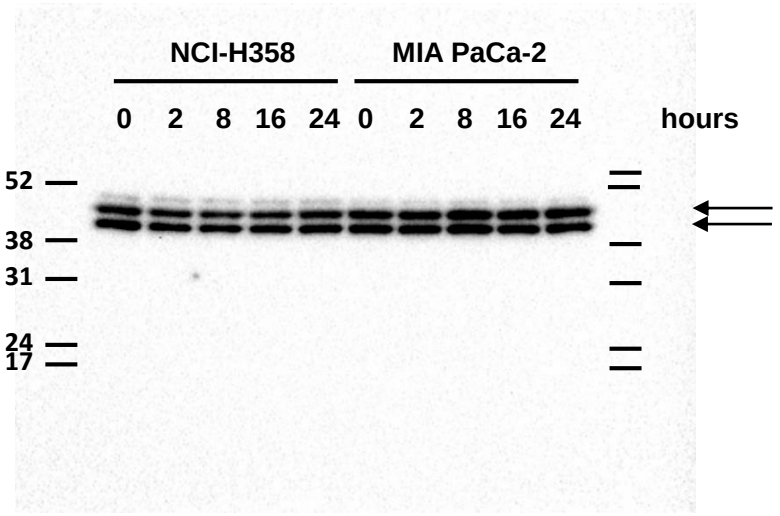

ERK1/2

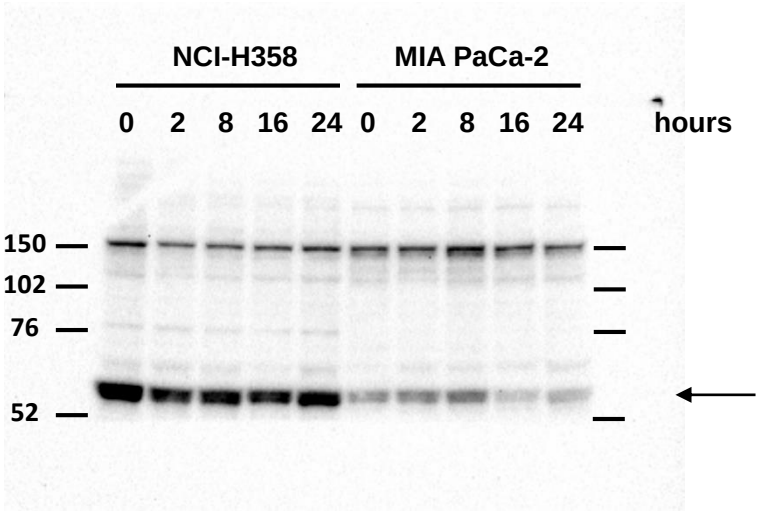

p-AKT S473

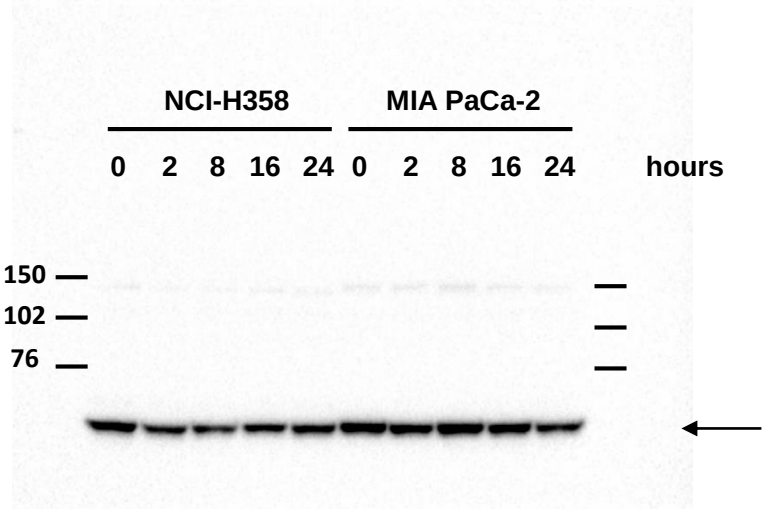

AKT

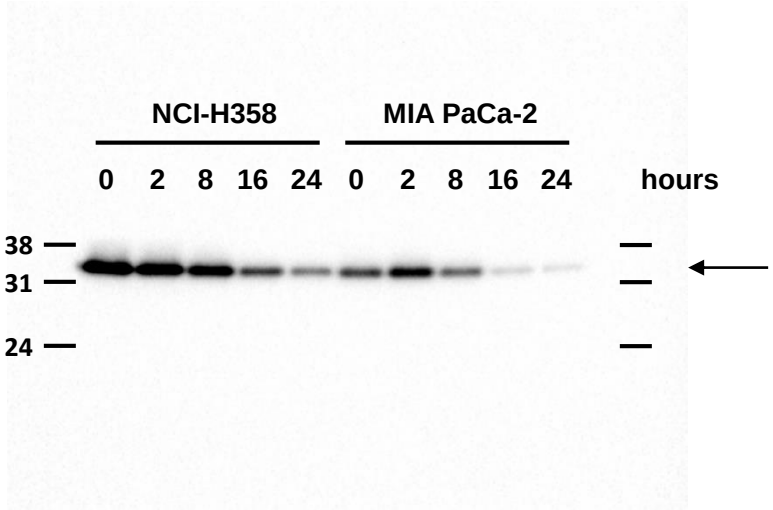

p-S6 S235/236

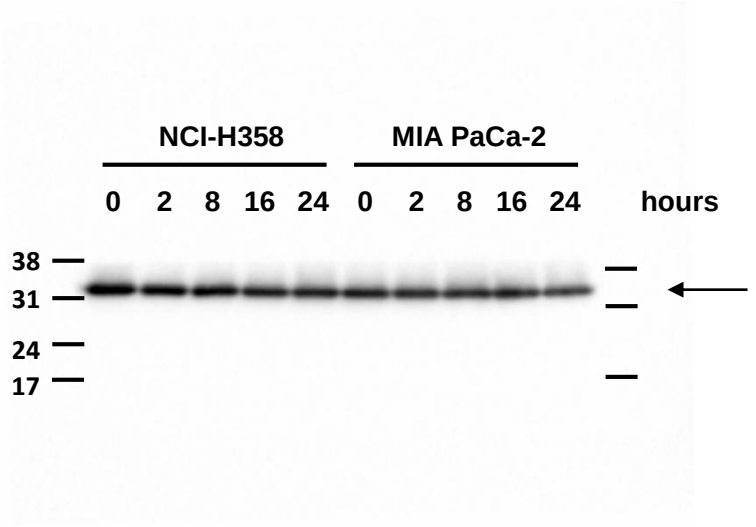

S6

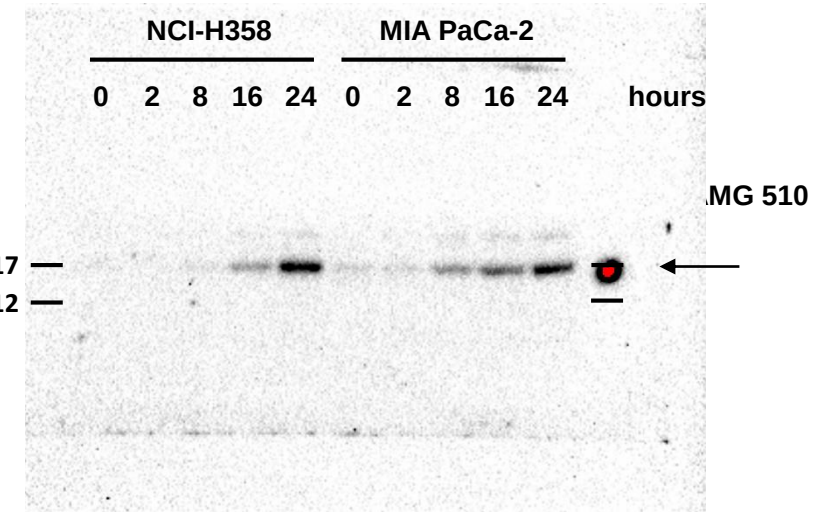

cleaved caspase-3

Supplementary Figure 1c (cont'd)

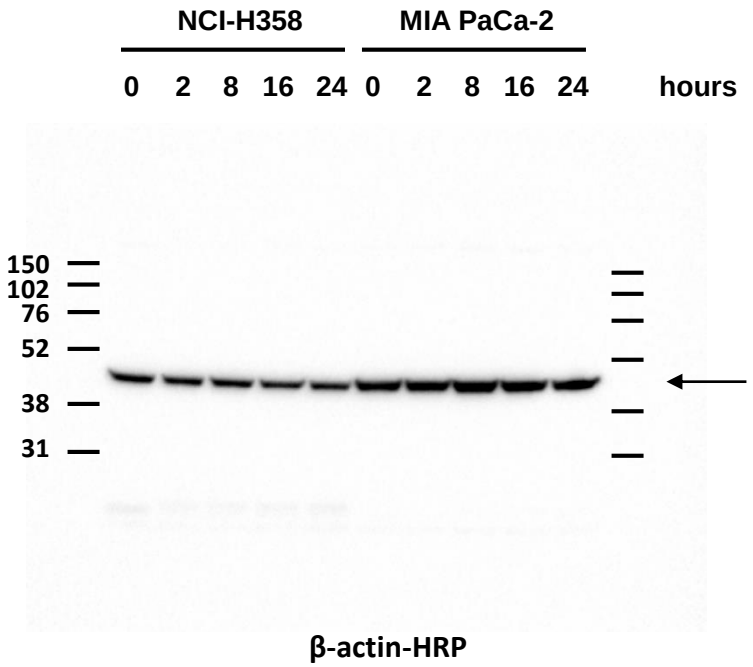

Supplementary Figure 1. Immunoblot source images for Extended Data Fig. 2b, c

a, Uncropped source images for immunoblots of lysates from NCI-H358 and MIA PaCa-2 cells treated with a dose titration of AMG 510 for 4 hours (Extended Data Fig. 2b). Beta-actin control was run on the same membrane used for the RAS immunoblot. **b**, Uncropped source images for immunoblots of lysates from NCI-H358 and MIA PaCa-2 cells treated with a dose titration of AMG 510 for 24 hours (Extended Data Fig. 2b). Beta-actin control was run on the same membrane used for the RAS immunoblot. **c**, Uncropped source images for immunoblots of lysates from NCI-H358 and MIA PaCa-2 cells treated with 0.1 µM AMG 510 for 0, 2, 8, 16, or 24 hours (Extended Data Fig. 2c). Beta-actin control was run on the same membrane used for the RAS immunoblot.

Supplementary Figure 2. Gating strategies for Fig. 5a and Extended Data Fig. 9a

Lymphoid:

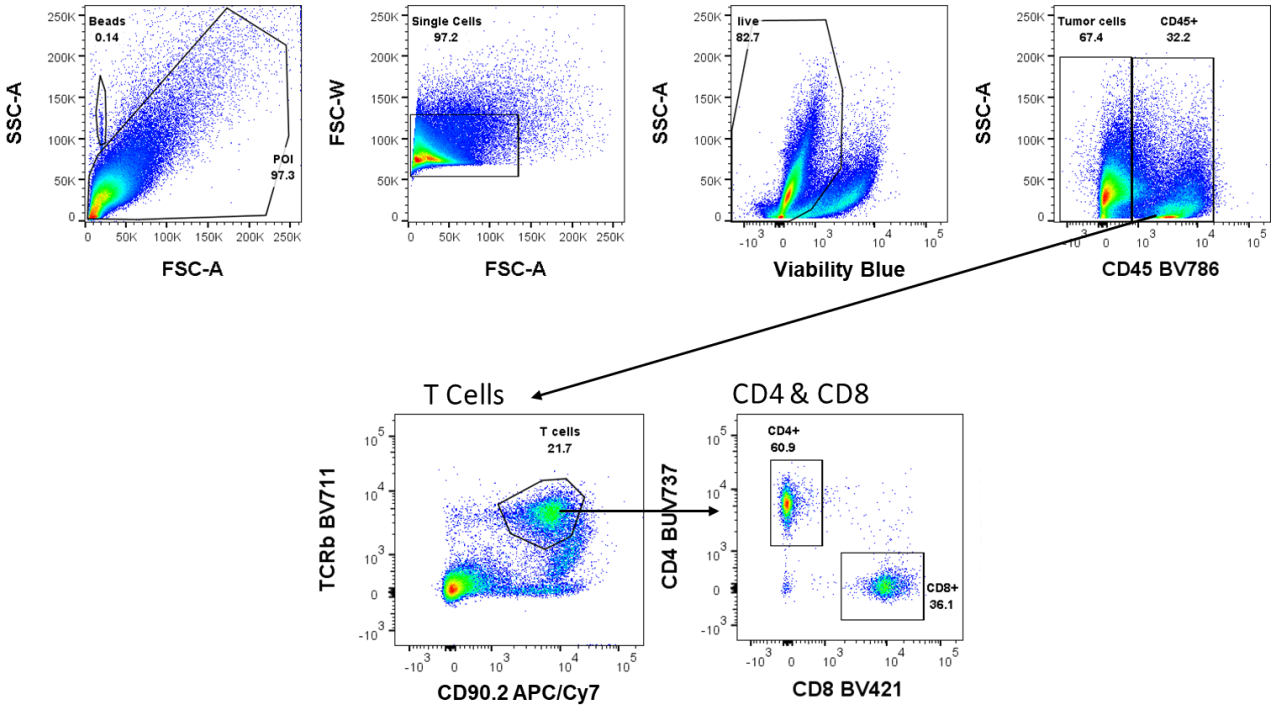

Myeloid:

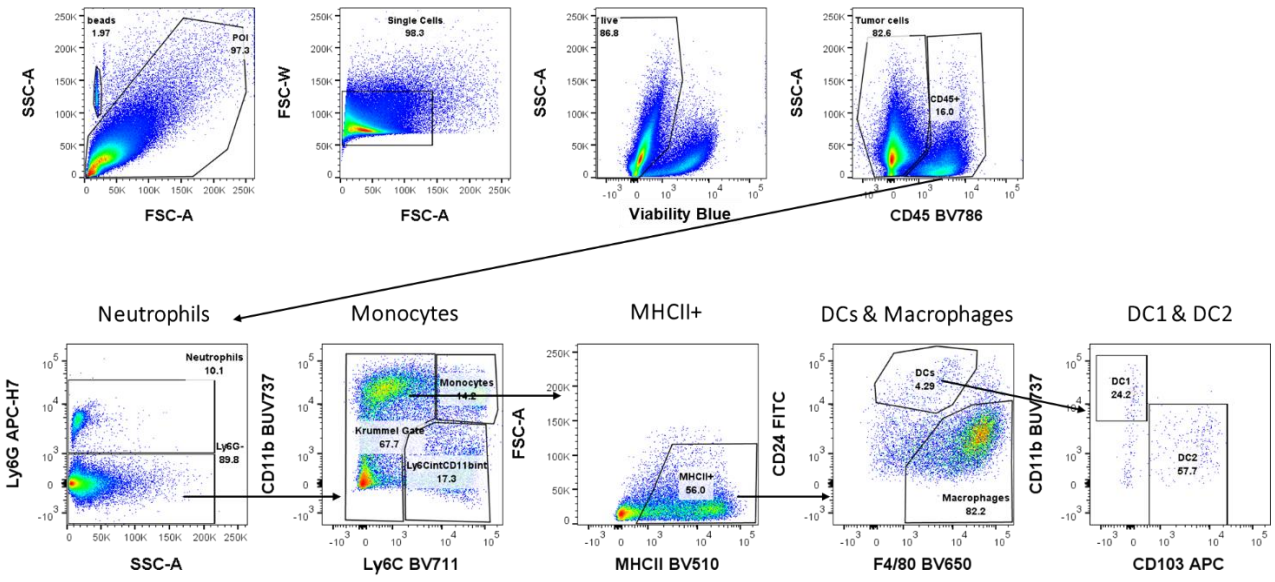

Supplementary Figure 3. Gating strategy for Fig. 5e and Extended Data Fig. 10c

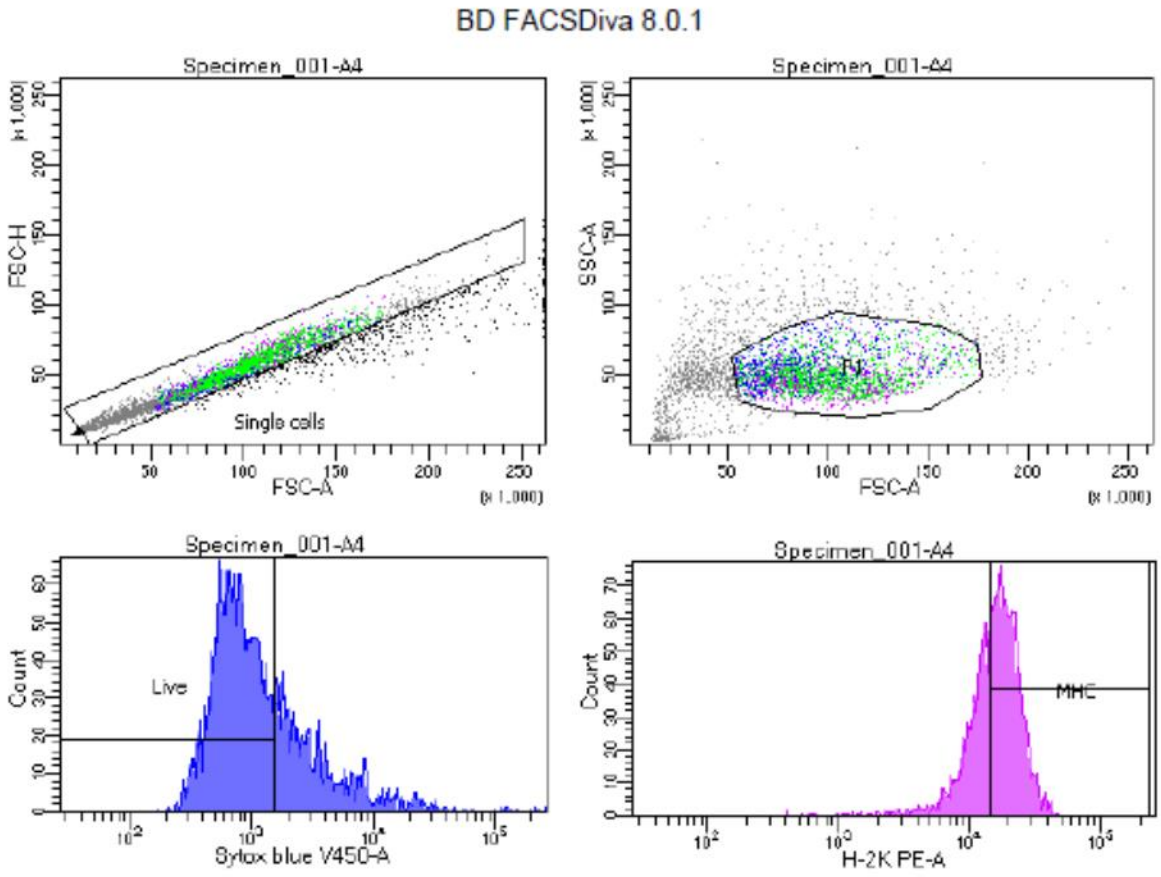

Well: A4

Population	#Events	%Parent	%Total
All Events	5,028	####	100.0
Single cells	4,118	81.9	81.9
P1	2,778	67.5	55.3
Live	1,880	67.7	37.4
MHC	1,089	57.9	21.7

Experiment Name:	20190205_kgaida_CT26_G12C...
Specimen Name:	Specimen_001
Record Date:	Feb 6, 2019 12:57:03 PM
Well Name:	A4

Population	#Events	%Parent	Sytox ... Geo M...	Sytox ... Mean	Sytox ... Median	H-2K ... Mean
Live	1,880	67.7	690	750	693	15,997
P1	####	####	1,238	3,882	939	16,481

Supplementary Figure 4. Gating strategy for Extended Data Fig. 10b

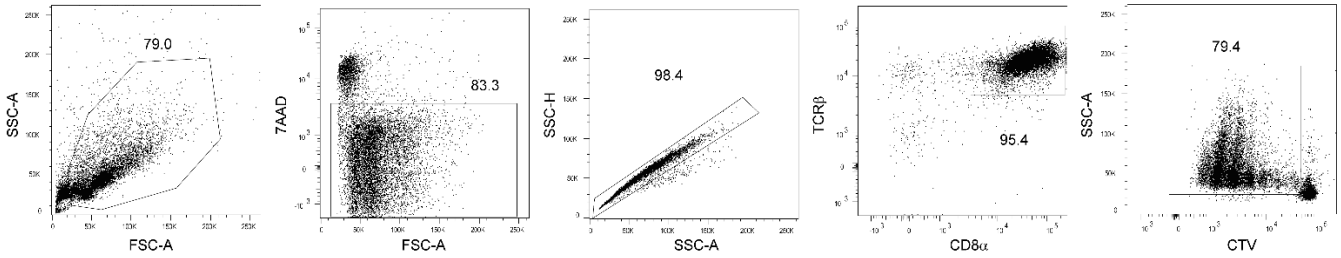

Supplementary References

1 Ostrem, J. M., Peters, U., Sos, M. L., Wells, J. A. & Shokat, K. M. K-Ras(G12C) inhibitors allosterically control GTP affinity and effector interactions. *Nature* **503**, 548-551, doi:10.1038/nature12796 (2013).

2 Barrett, S. D. *et al.* The discovery of the benzhydroxamate MEK inhibitors CI-1040 and PD 0325901. *Bioorganic & medicinal chemistry letters* **18**, 6501-6504, doi:10.1016/j.bmcl.2008.10.054 (2008).

3 Norman, M. H. *et al.* Selective class I phosphoinositide 3-kinase inhibitors: optimization of a series of pyridyltriazines leading to the identification of a clinical candidate, AMG 511. *Journal of medicinal chemistry* **55**, 7796-7816, doi:10.1021/jm300846z (2012).

4 Liang, S. C. *et al.* Regulation of PD-1, PD-L1, and PD-L2 expression during normal and autoimmune responses. *European journal of immunology* **33**, 2706-2716, doi:10.1002/eji.200324228 (2003).

5 Otwinowski, Z. & Minor, W. Processing of X-ray diffraction data collected in oscillation mode. *Methods in enzymology* **276**, 307-326 (1997).

6 Winn, M. D. *et al.* Overview of the CCP4 suite and current developments. *Acta crystallographica. Section D, Biological crystallography* **67**, 235-242, doi:10.1107/S0907444910045749 (2011).

7 Vagin, A. T., A. . MOLREP: an Automated Program for Molecular Replacement. *J. Appl. Crystallogr.* **30**, 1022-1025 (1997).

8 Murshudov, G. N. *et al.* REFMAC5 for the refinement of macromolecular crystal structures. *Acta crystallographica. Section D, Biological crystallography* **67**, 355-367, doi:10.1107/S0907444911001314 (2011).

9 Emsley, P. & Cowtan, K. Coot: model-building tools for molecular graphics. *Acta crystallographica. Section D, Biological crystallography* **60**, 2126-2132, doi:10.1107/S0907444904019158 (2004).

10 Schuttelkopf, A. W. & van Aalten, D. M. PRODRG: a tool for high-throughput crystallography of protein-ligand complexes. *Acta crystallographica. Section D, Biological crystallography* **60**, 1355-1363, doi:10.1107/S0907444904011679 (2004).

11 Saiki, A. Y. *et al.* MDM2 antagonists synergize broadly and robustly with compounds targeting fundamental oncogenic signaling pathways. *Oncotarget* **5**, 2030-2043, doi:10.18632/oncotarget.1918 (2014).

12 Campuzano, I. D. *et al.* High-Throughput Mass Spectrometric Analysis of Covalent Protein-Inhibitor Adducts for the Discovery of Irreversible Inhibitors: A Complete Workflow. *Journal of biomolecular screening* **21**, 136-144, doi:10.1177/1087057115621288 (2016).

13 Patricelli, M. P. *et al.* Selective Inhibition of Oncogenic KRAS Output with Small Molecules Targeting the Inactive State. *Cancer discovery* **6**, 316-329, doi:10.1158/2159-8290.CD-15-1105 (2016).

14 Ting, L., Rad, R., Gygi, S. P. & Haas, W. MS3 eliminates ratio distortion in isobaric multiplexed quantitative proteomics. *Nature methods* **8**, 937-940, doi:10.1038/nmeth.1714 (2011).

15 McAlister, G. C. *et al.* MultiNotch MS3 enables accurate, sensitive, and multiplexed detection of differential expression across cancer cell line proteomes. *Analytical chemistry* **86**, 7150-7158, doi:10.1021/ac502040v (2014).

16 Paulo, J. A. *et al.* Quantitative mass spectrometry-based multiplexing compares the abundance of 5000 S. cerevisiae proteins across 10 carbon sources. *Journal of proteomics* **148**, 85-93, doi:10.1016/j.jprot.2016.07.005 (2016).

17 Tomfohr, J., Lu, J. & Kepler, T. B. Pathway level analysis of gene expression using singular value decomposition. *BMC Bioinformatics* **6**, 225, doi:10.1186/1471-2105-6-225 (2005).

18 Tate, J. G. *et al.* COSMIC: the Catalogue Of Somatic Mutations In Cancer. *Nucleic Acids Res* **47**, D941-D947, doi:10.1093/nar/gky1015 (2019).
19 Misale, S. *et al.* KRAS G12C NSCLC Models Are Sensitive to Direct Targeting of KRAS in Combination with PI3K Inhibition. *Clinical cancer research : an official journal of the American Association for Cancer Research* **25**, 796-807, doi:10.1158/1078-0432.CCR-18-0368 (2019).
20 Nightingale, K. *et al.* High-Definition Analysis of Host Protein Stability during Human Cytomegalovirus Infection Reveals Antiviral Factors and Viral Evasion Mechanisms. *Cell host & microbe* **24**, 447-460.e411, doi:10.1016/j.chom.2018.07.011 (2018).